AD-A119 511 DAVID W TAYLOR NAVAL SHIP RESEARCH AND DEVELOPMENT CE--ETC F/G 20/4
THE EFFECTS OF HULL PITCHING MOTIONS AND WAVES ON PERIODIC PROP--ETC(U)
SEP 82 S D JESSUP, R J BOSWELL

UNCLASSIFIED DTNSRDC-82/093 NL

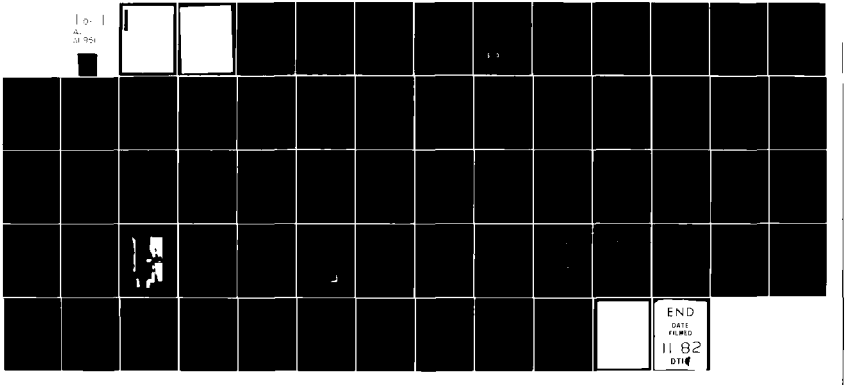

UNCLASSIFIED

SECURITY CLASSIFICATION OF THIS PAGE (When Data Entered)

REPORT DOCUMENTATION PAGE		READ INSTRUCTIONS BEFORE COMPLETING FORM
1. REPORT NUMBER DTNSRDC-82/093	2. GOVT ACCESSION NO. AD-A119511	3. RECIPIENT'S CATALOG NUMBER
4. TITLE (and Subtitle) THE EFFECTS OF HULL PITCHING MOTIONS AND WAVES ON PERIODIC PROPELLER BLADE LOADS		5. TYPE OF REPORT & PERIOD COVERED Final 6. PERFORMING ORG. REPORT NUMBER
7. AUTHOR(s) Stuart D. Jessup Robert J. Boswell		8. CONTRACT OR GRANT NUMBER(s)
9. PERFORMING ORGANIZATION NAME AND ADDRESS David W. Taylor Naval Ship Research and Development Center Bethesda, Maryland 20084		10. PROGRAM ELEMENT, PROJECT, TASK AREA & WORK UNIT NUMBERS Task Area S0379-SL001 Task 19977 Work Unit 1544-350
11. CONTROLLING OFFICE NAME AND ADDRESS Naval Sea Systems Command (05R) Ship Systems Research and Technology Group Washington, D.C. 20362		12. REPORT DATE September 1982 13. NUMBER OF PAGES 62
14. MONITORING AGENCY NAME & ADDRESS(if different from Controlling Office) Naval Sea Systems Command (56X4) Propulsion Lineshaft Equipment Division Washington, D.C. 20362		15. SECURITY CLASS. (of this report) UNCLASSIFIED 15a. DECLASSIFICATION/DOWNGRADING SCHEDULE

16. DISTRIBUTION STATEMENT (of this Report)

APPROVED FOR PUBLIC RELEASE: DISTRIBUTION UNLIMITED

17. DISTRIBUTION STATEMENT (of the abstract entered in Block 20, if different from Report)

18. SUPPLEMENTARY NOTES

Presented at the Fourteenth Symposium on Naval Hydrodynamics, The University of Michigan, Ann Arbor, Michigan, 23-27 August 1982.

19. KEY WORDS (Continue on reverse side if necessary and identify by block number)

Marine Propeller
Loads
Propulsion
Model Experiments
Propeller Research
Unsteady Loads
Waves
Dynamic Pitching

20. ABSTRACT (Continue on reverse side if necessary and identify by block number)

Fundamental investigations were made of the effects of periodic hull pitching motions and waves on the periodic loads on propeller blades and bearings. These periodic loads were measured during carefully controlled model experiments in which the periodic hull pitching motions, regular waves, and relative phase of the hull pitching to the wave encounter were systematically and independently varied. The periodic blade loads were calculated

(Continued on reverse side)

DD FORM 1 JAN 73 1473 EDITION OF 1 NOV 65 IS OBSOLETE
S/N 0102-LF-014-6601

UNCLASSIFIED
SECURITY CLASSIFICATION OF THIS PAGE (When Data Entered)

(Block 20 continued)

using trochoidal wave velocity profiles, and representation of the propeller based on a quasi-steady method.

The results of both theory and experiment show significant modulation of the amplitudes of the periodic blade loads with hull pitching motions and wave frequency of encounter. Further, the experiments confirm the theoretical assumption that the individual influences of the wave velocity profile and the induced velocities due to vertical hull motions can be linearly superimposed. The influence of the hull significantly modifies the amount of modulation of the shaft frequency loads due to both the periodic vertical motion of the propeller and the trochoidal wave velocity profile in the absence of the hull. However, trends of shaft frequency loads are well predicted by simple periodic variations of the velocity into the propeller, and a simple quasi-steady representation of the propeller. Trends of the results are shown to be consistent with available full-scale data. Therefore, for engineering purposes, the modulation of blade loads due to waves and hull motions for transom type hulls can be estimated by simple trochoidal wave velocity profiles, quasi-steady propeller theory, and constant multiples derived from the experiments presented in this paper.

TABLE OF CONTENTS

	Page
LIST OF FIGURES	iv
LIST OF TABLES	v
ABSTRACT	1
INTRODUCTION	1
EXPERIMENTAL TECHNIQUES	4
DYNAMOMETRY	4
HULL PITCHING AND WAVE SIMULATION	4
EXPERIMENTAL CONDITIONS AND PROCEDURES	5
DATA ACQUISITION AND ANALYSIS	7
ACCURACY	8
DISCUSSION OF EXPERIMENTAL RESULTS	9
LOADING COMPONENTS	9
CENTRIFUGAL AND GRAVITATIONAL LOADS	10
INFLUENCE OF DYNAMOMETER BOAT	10
OPERATION IN CALM WATER WITHOUT HULL PITCHING	11
OPERATION IN CALM WATER WITH HULL PITCHING	13
Time-Average Loads Per Propeller Revolution	17
Periodic Loads	17
Peak Loads	18
OPERATION IN WAVES WITHOUT HULL PITCHING	19
Time-Average Loads Per Revolution	23
Periodic Loads	23
Peak Loads	24
OPERATION IN WAVES WITH HULL PITCHING	25
DISCUSSION	28
SUMMARY AND CONCLUSIONS	29
ACKNOWLEDGMENTS	30
REFERENCES	30
NOTATION	32

LIST OF FIGURES

Page

1 - Hull and Propeller Geometry 34

2 - Components of Blade Loading 35

3 - Hull and Dynamometer Boat 36

4 - Block Diagram of SERVOMECHANISM for Pitching Model at Specified Phase Relative to Waves 37

5 - Experimental Data Showing Plus and Minus 1.96 Standard Deviations on Measured Values of F_x 37

6 - Distribution of Wake in Propeller Plane 37

7 - Open-Water Characteristics of DTNSRDC Model Propellers 4710 and 4711 38

8 - Influence of Extraneous Signals on Measured Loads 38

9 - Experimental Data Showing Extraneous Higher Harmonics 39

10 - Variation of Experimental Hydrodynamic Loads with Angular Position for Simulated Propulsion in Calm Water without Hull Pitching 39

11 - Variations of Hydrodynamic Loads with Hull Pitch Cycle for Operation in Calm Water 40

12 - Variation of F_x with Blade Angular Position for Hull Pitching in Calm Water Showing Portions of the Hull Pitch Cycle with Extremes of Peak Loading 41

13 - Afterbody of Hull Showing Propeller Disk 41

14 - Variations of the Harmonic Amplitudes of F_x During the Hull Pitch Cycle in Calm Water 42

15 - Variations of Hydrodynamic Loads with Location in Wave Cycle for Operation Without Hull Pitching 43

16 - Variation of F_x with Blade Angular Position for Operation in Waves Without Hull Pitching Showing Selected Locations in Wave Cycle Illustrating Extremes of Variation in Loading 44

17 - Variations of Harmonic Amplitudes of F_x During Wave Cycle Without Hull Pitching 45

Page

18 - Comparison of Hydrodynamic Blade Loads for Operation in Waves with Hull Pitching with Values Obtained from Linear Superposition of Increases due to Pitching Only and Increases Due to Waves Only 46

19 - Maximum Absolute Values of Blade Loads for Various Values of Ψ_A, ζ_A/L_{PP} and $\Phi_\zeta - \Phi_\psi$ Derived from Linear Superposition of Increases due to Pitching Only and Increases due to Waves Only 48

LIST OF TABLES

1 - Experimental Conditions 49

2 - Time-Average Hydrodynamic Loads for Operation in Calm Water without Hull Pitching 49

3 - Comparison of Measured F_x with Other Transom-Stern Configurations for Operation in Calm Water with Hull Pitching 50

4 - Summary of Maximum Values of Hydrodynamic Loads for Operation in Calm Water with Hull Pitching 51

5 - Summary of Maximum Values of Hydrodynamic Loads for Operation in Waves without the Hull Pitching 52

THE EFFECTS OF HULL PITCHING MOTIONS AND WAVES ON PERIODIC PROPELLER BLADE LOADS

Stuart D. Jessup and Robert J. Boswell
David W. Taylor Naval Ship Research and Development Center
Bethesda, Maryland 20084

ABSTRACT

Fundamental investigations were made of the effects of periodic hull pitching motions and waves on the periodic loads on propeller blades and bearings. These periodic loads were measured during carefully controlled model experiments in which the periodic hull pitching motions, regular waves, and relative phase of the hull pitching to the wave encounter were systematically and independently varied. The periodic blade loads were calculated using trochoidal wave velocity profiles, and representation of the propeller based on a quasi-steady method.

The results of both theory and experiment show significant modulation of the amplitudes of the periodic blade loads with hull pitching motions and wave frequency of encounter. Further, the experiments confirm the theoretical assumption that the individual influences of the wave velocity profile and the induced velocities due to vertical hull motions can be linearly superimposed. The influence of the hull significantly modifies the amount of modulation of the shaft frequency loads due to both the periodic vertical motion of the propeller and the trochoidal wave velocity profile in the absence of the hull. However, trends of shaft frequency loads are well predicted by simple periodic variations of the velocity into the propeller, and a simple quasi-steady representation of the propeller. Trends of the results are shown to be consistent with available full-scale data. Therefore, for engineering purposes, the modulation of blade loads due to waves and hull motions for transom type hulls can be estimated by simple trochoidal wave velocity profiles, quasi-steady propeller theory, and constant multiples derived from the experiments presented in this paper.

I. INTRODUCTION

The mechanisms by which rough seas and resulting ship motions influence the time-average and periodic loads on propeller blades and propeller shafts and bearings are complex. Factors include the increased time-average propeller loading due to increased hull resistance and the increased periodic loading resulting from the influence of the

free surface and modification of the flow pattern into the propeller disk. This flow pattern is influenced by (1) direct orbital velocities from the ocean waves, (2) relative velocities of the propeller due to ship motions, and (3) modification of the hull wake pattern due to the ship motions in the rough sea.

In general, the rough sea modulates the amplitudes of the periodic loadings on the propeller blades and bearings from the corresponding values in calm water. The periodic loads on individual blades, including modulation by a rough sea, must be considered in the design of the propeller blades from consideration of fatigue. This is especially important for controllable pitch (CP) propellers. Periodic bearing forces, including modulation by a rough sea, are important for consideration of ship vibration, especially in the main propulsion system, noise, and fatigue strength of components of the main propulsion system. Extreme modulation of the periodic thrust in the main propulsion shafting can result in reversals of the thrust on the main thrust bearing which can cause extensive damage.

Procedures for calculating periodic propeller blade and bearing loads in calm water are reasonably well refined. These procedures have been summarized by Boswell et al. (1968, 1981), Breslin (1972), and Schwanecke (1975).

Procedures for calculating the blade and bearing loads in a seaway are much less refined than for steady operation in calm water. Lipis (1975) and Tasaki (1975) review the mechanisms and procedures for predicting the effect of the seaway on periodic bearing forces which, in principle, also apply to unsteady loading on an individual blade. Keil et al. (1972), Watanabe et al. (1973), and Lipis (1975) present data from strain measurements on the blades of full-scale propellers in both calm and rough seas. Gray (1981) presents the modulation of blade rate hull vibration due to ship motion in a seaway.

These existing data and procedures provide valuable information regarding increases in periodic blade and bearing loads due to operation in a seaway. However, they address the overall complex problem in a statistical manner including the net influence of a complex sea state, complex ship responses, and numerous interactions. However, to the authors' knowledge, before the present study there were no experimental measurements of periodic loads on individual propeller blades that demonstrated the influence of waves and ship motions in a controlled environment.

An extensive systematic model experimental program was undertaken to obtain fundamental information on the influences of rough water and ship motions on periodic propeller blade loads on high speed open-shaft transom stern configurations. The experiments were conducted under carefully controlled idealized conditions in which sinusoidal hull pitching motions and regular head waves were independently varied. Experiments with hull pitching were conducted on three hull forms, two of which were reported previously by Boswell et al. (1976a, 1976b, 1978) and Jessup et al. (1977), and the third of which is presented in this paper. Restrained model experiments in waves, including forced sinusoidal pitching of a model in waves, were conducted on only one model, and are presented in the present paper. Experiments were conducted in

calm water with no ship motions, in calm water with forced sinusoidal pitching of the hull, in regular waves with no ship motions, and in regular waves with forced sinusoidal pitching of the hull at the frequency equal to the wave frequency of encounter. The experiments with forced hull pitching in waves were run over a range of relative phases between the hull pitching and the wave encounter. Six components of blade loads were measured during the dynamic conditions simulated.

The modulation of the blade load variation was correlated with predictions calculated from trochoidal wave theory and the periodic vertical motion of the hull. The assumption of superposition of the effects of pitching and waves was evaluated. Trends of modulations of the periodic bearing loads were determined from the modulations of the pertinent harmonics of the single-blade loads.

The objective of these experiments was to obtain accurate systematic experimental data showing the effects of hull pitching and waves on periodic and time-average blade loads under carefully controlled experimental conditions so that the effects of ship motions and waves on periodic and time-average blade loads could be isolated. It is anticipated that these data will serve as a basis for developing procedures for calculating periodic and time-average blade loads for operation in a complex sea state.

In these experiments the model speed and propeller rotational speed were held constant at the values corresponding to operation in calm water with no ship motions. In practice, when a ship operates in rough seas the ship speed and propeller rotational speed at a given delivered power decrease from the corresponding values in calm water due to increased shaft torque resulting from increased resistance of the hull and change in the propulsion coefficients (involuntary speed loss) (Lewis, 1967, Oosterveld, 1978, Day et al., 1977). Furthermore, in rough seas the delivered power is often deliberately reduced from the calm water value (voluntary speed loss) as discussed by Day et al. (1977) and Lloyd and Andrew (1977). Therefore, the difference in blade loads between operation in calm seas and operation in rough seas can be represented as being made up of two major parts:

1. Differences in loads resulting from the difference in ship speed and propeller rotational speed between calm seas and rough seas, and

2. Increases in loads due to the direct influence of waves and ship motions at a given value of ship speed and propeller rotational speed.

The changes in propeller rotational speed, ship speed, and Taylor wake fraction due to operation in rough seas can be estimated experimentally or theoretically using methods or data summarized by Oosterveld (1978), Day et al. (1977), and Lloyd and Andrew (1977). The resulting changes in periodic blade loads can be estimated based on the systematic experimental data or theoretical methods described previously by Boswell et al. (1976a, 1976b, 1978). The experiments described in the present paper provide information on the direct influence of the waves and ship motions on periodic and time-average blade loads.

II. EXPERIMENTAL TECHNIQUES

A. Dynamometry

All experiments were conducted using the hull and propeller shown in Figure 1 on Carriage II at the David W. Taylor Naval Ship Research and Development Center (DTNSRDC), using basically the same dynamometry and hardware described by Boswell et al. (1976a, 1976b, 1978). The starboard propeller, on which blade loads were measured, was located its proper position relative to the model hull but was isolated from the hull and driven from downstream (see Figure 2). This downstream drive system was necessary in order to house instrumentation required obtain the frequency response characteristics of the system for measuring unsteady loading.

The sensing elements were flexures to which bonded semi-conductor strain-gage bridges were attached. The design of these flexures has been described by Dobay (1971). Three flexures were necessary to measure all six components of force and moment. Flexure 1 measured F_x and M_y, Flexure 2 measured F_y and M_x, and Flexure 3 measured F_z and M_z; see Figure 3. The flexures were mounted inside a propeller hub specifically designed for these experiments. Only one flexure could be mounted at a time because of space limitations, and this necessitated three duplicate runs for each condition. The flexure calibration procedure was identical to that described by Boswell et al. (1976a, 1976b, 1978).

The port propeller, on which blade loads were not measured, was driven from inside the model hull as would be the case in a self-propulsion experiment. The propeller rotational speed, which could be controlled independently of the starboard propeller, was measured via a toothed gear pickup and recorded on a digital voltmeter. The time-average thrust and torque were measured for selected runs by a transmission dynamometer.

B. Hull Pitching and Wave Simulation

The downstream body which housed the drive system was modified from the configuration used by Boswell et al. (1976a, 1976b, 1978) so that it could be operated fully submerged. This was necessary in the present experiment because the large shaft angle necessitated deep submergence, and the operation in waves caused an additional disturbance to the water surface. The modifications included a waterproof housing for the drive motor, waterproof electrical cables and connectors, removal of the upper apron which had extended the sides of the boat, and the addition of a nonwaterproof top to the boat. Both the body housing (the drive system was soft mounted to this body) and the model hull were rigidly attached to a pitch-heave oscillator which was driven by a hydraulic cylinder. The pitch-heave oscillator was rigidly mounted on the towing carriage. This arrangement enabled the model hull and the drive system to be dynamically pitched together while maintaining independent support from one another.

For operation in waves, regular head waves were generated by a pneumatic wavemaker (Brownell et al., 1956). The level of the water surface was measured as a function of time by a pulsed ultrasonic probe that was mounted on the carriage; see Figure 4. The output of this probe, which was filtered using a low pass filter to remove the influence of small irregularities in the water surface, yielded the amplitude and frequency of encounter of the wave.

For operation with forced dynamic pitching of the model hull in waves, a servomechanism was used to ensure that the pitching of the model hull maintained the desired phase relative to the wave at the propeller throughout the experimental run. Figure 4 presents a schematic diagram of this servomechanism. In this servomechanism, a servo-control unit subtracts the feedback signal from the hydraulic cylinder, e_p, from the signal from the wave height probe, e_w, and sends this difference signal, or servo signal e_s, to the servo valve. Based on this servo signal, e_s, the servo valve slightly adjusts the frequency of the hydraulic cylinder so that e_s seeks the null signal. When e_s is null, e_p is in phase with e_w; that is, the pitching is in phase with the waves. With this system small corrections to the frequency of the hydraulic cylinder are made continuously to maintain e_s near the null, and thus to maintain the pitching of the model in phase with the waves. The phase of the wave at the propeller plane was varied relative to the phase of the model pitching by moving the wave height probe used in the servomechanism forward or aft a prescribed distance relative to the plane of the propeller. For example, for setting the phase of the pitching, Φ_ψ, equal to the phase of the wave at the propeller plane, Φ_ζ, the wave height probe was placed in the propeller plane. For setting $\Phi_\zeta - \Phi_\psi = 90$ degrees, the wave height probe was placed a three-quarters of a wavelength forward of the propeller plane.

A second wave height probe, which was not used in the servomechanism, remained in the propeller plane for all conditions. The output of this probe was input for the computer and served as a reference for analyzing the blade force and moment data as a function of position in the wave cycle. In all cases, the wave height probes were placed sufficiently far from the model in the transverse plane so that the model did not disturb the water surface at the points at which the water levels were measured.

C. Experimental Conditions and Procedures

Experiments were conducted at several conditions including steady ahead operation in calm water with no ship motions, simulated periodic pitching of the hull in calm water, operation in regular head waves without pitching of the hull, and operation in regular head waves with periodic pitching of the hull. All conditions were run with the model hull rigidly attached to its support, with no freedom to sink or trim, and with essentially equal rotation on the port and starboard propellers.

The basic condition, which simulates steady ahead self-propulsion in calm water with no ship motions, is defined as Condition 1 in Table 1. The propeller rotational speed, trim and draft at this condition were obtained from model self-propulsion data. No cavitation occurred on the model propeller at any model experimental condition described in this paper.

Runs simulating hull pitching and/or the effect of waves were conducted at the same conditions as the run in calm water with no hull pitching, except that the hull pitch was varied and/or the model was run in waves (Conditions 2 to 6 in Table 1). These experiments were conducted for forced pitching of the model in calm water, for operation in regular head waves without pitching of the restrained model hull, and for forced pitching of the model for operation in regular head waves. For forced pitching in waves, the phase of the wave at the propeller, Φ_ζ, was varied relative to the phase of the hull pitching, Φ_ψ. Three relative phases were evaluated:

1. Wave crest at the propeller plane when the stern of the model hull is pitched up at its maximum value, $\Phi_\zeta - \Phi_\psi = 0$ (Condition 4 in Table 1).

2. Wave crest at the propeller plane when the stern of the model hull is pitched down at its maximum value, $\Phi_\zeta - \Phi_\psi = 180$ degrees (Condition 5 in Table 1).

3. Wave crest at the propeller planes when the hull pitch is passing through its mean value $(\psi_{MAX} - \psi_{MIN})/2$ from stern down to stern up, $\Phi_\zeta - \Phi_\psi = 90$ degrees (Condition 6 in Table 1).

For the unsteady hull-pitch simulation in calm water, the hull-pitch angle ψ was varied sinusoidally about the calm water equilibrium trim angle (ψ_{CW}) with an amplitude ψ_A of 1.33 degrees and a frequency f_ψ of 0.8 hertz, $f_\psi L_{PP}^{1/2}/g^{1/2} = 2.63$. For operation in waves without the hull pitching, the model hull operated in regular head waves with a single amplitude ζ_A of 0.118 m (0.39 ft), $\zeta_A/L_W = 0.019$; a wavelength L_W of 9.20 m (30.20 ft), $L_W/L_M = 1.62$; and a wave velocity V_W of 3.79 m/s (12.43 ft/s). At the experimental model speed of 3.58 m/s (6.96 knots) the frequency of encounter is 0.8 hertz which is the same as the model pitching frequency. Operation in waves with pitching of the model hull necessitated a reduction in the amplitude of the pitch of the model hull and/or the amplitude of the waves from the aforementioned values in order to prevent flooding of the model hull. The minimum amplitudes of the hull pitch and the waves were 0.67 degree and 75 mm (0.25 ft), respectively (see Table 1). The frequency of the hull pitching and the frequency of encounter of the waves were both 0.8 hertz for all experimental conditions with pitching and waves.

The selected amplitude and frequency of encounter of the waves, and amplitude and frequency of the hull pitching were within the scaled, predicted operating and response characteristics at full scale of an equivalent transom-stern ship.

Air-spin experiments were conducted with all three flexures over a range of rotational speeds in order to isolate the effects of

centrifugal and gravitational loading from hydrodynamic loading. Supplemental experiments were conducted to assess the influence of the downstream dynamometer boat on the flow in the propeller plane. These supplemental experiments consisted of wake surveys in the propeller plane in calm water without the hull pitching (Condition 1 in Table 1) with and without the downstream body. These wake surveys yielded a direct measure of the change in the velocity distribution through the propeller disk attributable to the downstream body.

D. Data Acquisition and Analysis

Data were collected, stored, and analyzed on-line using a minicomputer. A computer program was written with options for analyzing each of the two basic types of runs: (1) operation in calm water without hull pitching, and (2) operating with periodic hull pitching and/or operation in regular waves. Data were collected and analyzed in the same manner as described by Boswell et al. (1976a, 1976b, 1978). For a given run, the computer collected force, moment, propeller rotation speed, model speed, hull pitch angle, and wave height at 4-degree increments of propeller angular position over 200 to 300 propeller revolutions.

For operation in calm water without hull pitching, the computer was used to analyze and print the data. The average force and moment signals for each 4-degree angular position were printed along with the average model velocity and propeller rotation speed for the run. The standard deviation of the accumulated data for the run was also calculated for V, n, and the force and moment signals at each position. A harmonic analysis was performed on the force and moment data providing the mean signal and amplitude and phase of the first 16 harmonics of shaft speed.

For runs simulating hull pitching or waves, the force and moment data were selectively analyzed over the range of pitch angles or wave heights measured. Initially, the values of pitch and wave height were averaged over each revolution of a given run. An analysis was used to search through a series of similar runs extracting propeller revolutions of force and moment data corresponding to prescribed values of pitch or wave height with a prescribed slope and tolerance band. Typically, 50 to 200 revolutions were averaged at each value of pitch or wave height. Twenty-six positions in the pitch or wave cycle were selected for analysis.

For runs with pitching in waves, both the pitch angle and the wave height were fed into the computer. The blade loading data could be sorted based on either of these two signals. To check the proper phasing between the two signals, the pitch and wave data were also analyzed in the time domain. For each run, a strip chart record of the pitch angle and wave height variation was printed, along with analysis of the average frequency, amplitude and phase of the two signals. Runs with consistent wave and pitching frequency, amplitude, and phases were selected for blade loading analysis.

Final analysis was conducted after the experimental agenda was repeated for each of the three flexures representing the six components of blade load. Corrections for interactions between the various load components were performed for a representative condition in calm water without hull pitching, as outlined by Boswell et al. (1976a, 1976b, 1978). The resulting load corrections were applied to all other conditions in the experimental agenda. The total loading components were corrected for the centrifugal and gravitational loads to obtain the hydrodynamic loads. Corrections were also made to the mean loads to account for the influence of the dynamometer boat.

E. Accuracy

The accuracy of the experiment was generally similar to that described by Boswell et al. (1976a, 1976b, 1978). During the experiments, the on-line analysis averaged data over many revolutions and computed standard deviations of speed V, rotation speed n, forces, and moments, assuming a normal distribution in the variation of these quantities. From this, a variation in the measured quantities was calculated with a 95 percent confidence level. Model speed V, and rotation speed n varied by ± 0.5 percent from calculated mean values. For the condition in calm water with no hull pitching, the force and moment signals at each angular position measured, varied by ± 2 to ± 10 percent of the calculated average value. Figure 5 shows the measured variation in the raw F_X signal. Note that the variation in force at each angular position was greatest when the blade was nearest the model hull. The variation of the loading components during the pitching and wave conditions was ± 10 to ± 20 percent of the mean values at each angular position. These variations were greater than the still water condition because each run was evaluated over a certain tolerance range in pitch or wave height. It should be noted that the variations from the mean represent the band in which 95 percent of the measured data lie. The accuracy of the mean values calculated will be higher than the variations calculated.

Besides the fluctuation in signals occurring in a given run, the overall accuracy of the data can be represented by the repeatability between different runs. An effort was made to set experimental conditions identically on repeat runs; however, the propeller rotational speed and model velocity were set by hand, so some variation was unavoidable. The variation in the measured experimental conditions and the blade loading data for repeat runs is similar to that documented by Boswell et al. (1978) and Jessup et al. (1977) showing that the variations in the mean forces and moments were ± 4 percent over all the runs.

As discussed in the section on data acquisition and analysis, for operation with periodic pitching either with or without waves, the data were sorted and analyzed based on instantaneous position in the pitch cycle, and for operation in waves without hull pitching, the data were sorted and analyzed based on instantaneous position of the propeller in the wave cycle. For periodic pitching runs, selection of a propeller revolution at a specified pitch angle ψ in the pitch cycle necessitated a tolerance of 0.05 degree to ψ; however, the average value of ψ for

which data were presented during the periodic pitching runs was generally within 0.02 degree of the target ψ. For runs in waves without hull pitching, the selection of a propeller revolution at a specified instantaneous water level within the wave necessitated a tolerance of 5 mm (0.20 in.) of the target water level.

Considering all sources of error including deviations during a run and inaccuracies in setting conditions, the model scale forces and moments presented in this paper are generally considered to be accurate to within (plus or minus) the following variations:

	$\overline{F}$		F_{MAX}		$\overline{M}$		M_{MAX}	
	N	(lb)	N	(lb)	N-m	(in-lb)	N-m	(in-lb)
Calm water without hull pitching	0.4	(0.1)	0.9	(0.2)	0.02	(0.2)	0.05	(0.4)
Pitching and/or waves	0.9	(0.2)	1.8	(0.4)	0.05	(0.4)	0.09	(0.8)

The values are somewhat more accurate for the runs in calm water without pitching than for runs with pitching and/or waves, because the experimental conditions could be controlled more precisely for runs in calm water without waves and the measured forces and moments were averaged over many more revolutions of the propeller. The time-average values per revolution (based on 90 samples per revolution) are slightly more accurate than the maximum values (based on one sample per revolution) which took into account the variation with blade angular position. Further, the peak values may have been slightly influenced by the dynamic response of the flexures.

III. DISCUSSION OF EXPERIMENTAL RESULTS

A. Loading Components

The basic loading components are shown in Figure 2. For a right-hand propeller, as used in this case, the sign convention follows the conventional right-hand rule with right-hand Cartesian coordinate system.

Each component of loading is represented as a variation of the instantaneous values with blade angular position, θ, and as a Fourier series in blade angular position in the following form:

$$F,M(\theta) = (\overline{F},\overline{M}) + \sum_{n=1}^{N} (F,M)_n \cos\{n\theta - (\phi_{F,M})_n\} \qquad (1)$$

In general, the loads consist of hydrodynamic, centrifugal and gravitational components. However, in this paper, only the hydrodynamic component of blade loading is presented. The results considering total loads showed the same trends as results including only hydrodynamic loads. Centrifugal and gravitational loads were measured to permit the hydrodynamic loads to be determined by subtracting the centrifugal and gravitational loads from the total experimental loads. The centrifugal and gravitational loads were, of course, independent of hull pitching and waves since all conditions were run at the same propeller rotational speed, n.

B. Centrifugal and Gravitational Loads

Centrifugal and gravitational loads were determined from air-spin experiments with each flexure over a range of rotational speed n. The centrifugal load, which is a time-average load in a coordinate system rotating with the propeller, should vary as n^2. The time-average experimental data followed this trend. The gravitational load, which is a first harmonic load in a coordinate system rotating with the propeller, should be independent of n. The first harmonic experimental data followed this trend.

The centrifugal and gravitational loads measured during these experiments agreed with the values determined by Boswell et al. (1981), and the gravitational loads agreed with values deduced from the weights of the blades and associated flexures. Therefore, these results will not be repeated here.

C. Influence of Dynamometer Boat

The results of the wake survey with and without the downstream body (dynamometer boat) are presented in Figure 6. Harmonic analysis of these data indicate that the downstream body had only a small effect on the circumferential and radial variations in the flow and only a small effect on the harmonic content of the flow. However, they also indicate that the downstream body reduced the volume mean speed through the propeller disk by approximately 12 percent. These results are, of course, without the propeller in place.

The change in effective speed through the propeller due to the downstream body was deduced from thrust and torque identities between the mean thrust and torque measured during the blade loading experiments and mean thrust and torque measured during the corresponding self-propulsion model-experiment. These results, which include the effect of the propeller, indicate that the downstream body reduced the effective speed through the propeller disk by approximately 14 percent; i.e., without the body, $(1-w_T) = 1.00$ and $(1-w_Q) = 1.00$, whereas, with the body, $(1-w_T) = 0.86$ and $(1-w_Q) = 0.85$. This agrees quite closely with the 12 percent reduction in the volume mean speed due to the downstream body as deduced from the wake surveys at the corresponding conditions.

Based on these results, it was concluded that the downstream body reduced the mean speed into the propeller by 14 percent for all conditions. These reductions are somewhat larger than the 12 and 5 percent reductions obtained by Boswell et al. (1976a, 1976b, 1978), respectively, in which essentially the same dynamometer boat was used behind other model hulls. However, in the earlier experiments the dynamometer boat was not fully submerged.

The downstream body will disturb the location of the shed and trailing vortex sheets from the propeller. This may influence the periodic and time-average propeller blade loads. No correction was made for this effect.

After the effects of centrifugal force were subtracted from the measured loading components as discussed previously, the time-average value per revolution of each hydrodynamic loading component was corrected for the downstream body as follows: From the measured hydrodynamic blade thrust ($\overline{F}_{x_H}$) and hydrodynamic blade torque ($\overline{M}_{x_H}$), effective advance coefficients based on thrust identity (J_T) and torque identity (J_Q) were deduced from the open water data (Figure 7). These values were multiplied by (1/0.88) to obtain corrected values of J_T and J_Q, i.e., without the downstream body. The corrected values of $\overline{F}_{x_H}$ and $\overline{M}_{x_H}$ were then obtained from the open water data at the corrected advance coefficient J_T and J_Q, respectively. It was assumed that the downstream body did not affect the radial centers of thrust $\overline{F}_{x_H}$ and tangential force $\overline{F}_{y_H}$. Therefore,

$$\overline{M}_{y_H} \text{ corrected} = (\overline{F}_{x_H} \text{ corrected}/\overline{F}_{x_H} \text{ measured}) \; (\overline{M}_{y_H} \text{ measured})$$

$$\overline{F}_{y_H} \text{ corrected} = (\overline{M}_{x_H} \text{ corrected}/\overline{M}_{x_H} \text{ measured}) \; (\overline{F}_{y_H} \text{ measured})$$

No corrections are made to F_{z_H} and M_{z_H} for the effect of the downstream body; however, $\overline{F}_{z_H}$, $\overline{M}_{z_H}$ are small for all experimental conditions, as discussed later.

No correction for the effect of the downstream dynamometer boat was made to the measured circumferential variations of the loading components. Calculations made by the methods of Tsakonas et al. (1974) and McCarthy (1961) indicated that the influence of the downstream body alters the peak-to-peak circumferential variation of the loads by no more than 2 percent.

D. Operation in Calm Water Without Hull Pitching

For operation in calm water without the hull pitching (Condition 1 in Table 1), Table 2 presents the time-average loads, Figure 8 presents the variation of the F_x component of hydrodynamic blade loading with blade angular position, and Figure 9 presents the amplitude of the first 25 harmonics of the F_x component of hydrodynamic blade loading.

Based on the dynamic calibration by Dobay (1971), it was judged that for all loading components the data are valid for the first 10

harmonics. In addition, the wake data show no significant amplitudes for harmonics greater than the tenth. Therefore, all data and analyses except Figures 8 and 9 are based on reconstructed signals using the first 10 harmonics. The symbols shown in Figure 8 indicate unfiltered values determined from the experiment; each represents the average value at the indicated blade angular position for over 200 propeller revolutions. The variation in measured values at a given angular position is discussed in the section on accuracy. The lines on Figure 8 indicate that the variations of the signals with blade angular position are adequately represented by the number of harmonics retained.

The variations of all measured hydrodynamic loading components with blade angular position for simulated propulsion in calm water without hull pitching are shown in Figure 10. The amplitudes and phases of the harmonics of these loading components are presented in Figure 9.

These data show that for hydrodynamic loading the variation of all loading components was predominantly a once-per-revolution variation. The extreme values for all loading components, except F_Z and M_Z, occurred near the angular position of the spindle axis, θ = 114 and 270 degrees; i.e., within 24 degrees of the horizontal. The propeller evaluated has a projected skew angle at the tip of approximately 11 degrees; therefore at the positions of extreme loading the blade tip is within approximately 13 degrees of the horizontal. This suggests that the tangential component of the wake is the primary driving force; see Figure 6. The extreme values of F_Z and M_Z occur within 20 degrees of the extreme values of the other components. The reason for this variation in location of extreme values is not clear; however, it may be partially due to experimental inaccuracy with the F_Z-M_Z flexure as discussed by Boswell et al. (1976a, 1976b, 1978). Further the net stresses in the blades are generally less sensitive to the F_Z and M_Z components than they are to the other force and moment components.

The results presented here for circumferential variation of hydrodynamic loads follow trends similar to results presented by Boswell et al. (1976a, 1976b) for a single-screw transom-stern configuration and results presented by Boswell et al.(1978) and Jessup et al. (1977) for a twin-screw transom-stern configuration.

The circumferential variations and first harmonics of all loading components except F_Z and M_Z were substantially larger fractions of their time-average values for the condition evaluated here than they were for the conditions evaluated previously on the models reported by Boswell et al. (1976a, 1976b, 1978). For example, $(\overline{F}_{x_H})_1/\overline{F}_{x_H}$ was 0.66 for the present case, 0.40 from Boswell et al.(1976), and 0.42 from Boswell et al. (1978). The differences in the ratios of the circumferential variations of loads to the time-average loads for these three cases arise from many factors including the propeller time-average loading coefficients which are essentially independent of the unsteady loading, the magnitude of the circumferential variation of the wake (primarily the amount of shaft inclination for the three cases under consideration here), and propeller geometry especially the blade width and pitch-diameter ratio. The ratio of the unsteady loading to the time-average loading is useful for evaluating the unsteady loading of a given

propeller over a range of ship and propeller operating conditions; however, this ratio is not a good parameter for comparing the unsteady loadings on different propellers on different ships with different operating conditions. Analytical calculations, not presented here, confirm that the periodic loading components for operation in calm water with no ship motions should be larger fractions of the respective time-average loading components for the propeller-hull combination described in the present paper than for those described by Boswell et al. (1976a, 1976b, 1978).

E. Operation in Calm Water with Hull Pitching

Figure 11 shows the variations of peak values per revolution, time-average values per revolution, and first harmonic values of the F_x and M_x components of hydrodynamic blade loading with hull pitch angle ψ (Condition 2 in Table 1). The F_y and M_y components showed similar variations as in Figure 11, and the F_z and M_z components were found to be relatively independent of hull pitch, and therefore are not shown. Table 4 summarizes the maximum absolute values of the peak loads, first harmonic loads, and time-average load per revolution for operation in calm water with hull pitching.

Figure 11 shows the loading components at the individual pitch angles analyzed. Spline curves were fit through the points shown. An oscillatory behavior is shown in the peak and first harmonic loads at the time when the hull is moving from stern-up to stern-down position. This behavior was believed to be caused by observed slight transverse oscillation of the dynamometer boat probably caused by vortex shedding. This did not occur in the experiments described by Boswell et al. (1976a, 1976b, 1978) because the dynamometer boat was not completely submerged in those experiments as it was in the present experiments. This behavior was believed to have no significance, since the model hull did not oscillate transversely in a similar fashion. Therefore, this oscillation is faired out in the curves shown in Figure 11.

The time-average values per revolution for each of the two loading components remained within 5 percent of their values in calm water without hull pitching throughout the pitch cycle presented. The trends in variations of the time-average values of the various components with position in the pitch cycle are similar. The largest absolute values of the time-average values per revolution of all loading components occurred near the time at which the hull pitch was passing through its equilibrium value from stern-up to stern-down; i.e., near $(\psi - \psi_{CW}) = 0$, $\dot{\psi} < 0$.

The maximum absolute values of the peak loads increased by as much as 22 percent relative to the time-average loads in calm water without hull pitching above the corresponding peak loads in calm water without hull pitching. Similarly, the maximum values of the first harmonic loads increased by as much as 13 percent relative to the time-average loads in calm water without hull pitching. The maximum absolute values of both the peak loads and the first harmonic loads for all components

occurred approximately over the angular positions of 145 to 230 degrees in the hull pitch cycle shown in Figure 11. This corresponds to the portion of the cycle in which the hull was passing through its equilibrium value from stern-up to stern-down; i.e., near $(\psi - \psi_{CW}) = 0$, $\dot{\psi} < 0$. This is the same portion of the pitch cycle during which the maximum time-average values per revolution occurred; therefore, the maximum increase in the time-average loads per revolution and the maximum increase in the unsteady loads per revolution tend to add (they are in phase relative to the hull pitch) to yield the maximum increase in peak loads. The smallest absolute values of time-average, peak loads, and first harmonic loads occurred near $\psi - \psi_{CW}$ as the hull passed from the stern-down to the stern-up portion of the cycle; i.e., $(\psi - \psi_{CW}) = 0$, $\dot{\psi} < 0$.

Figure 12 shows the variation of the F_x component with blade angular position for times in the pitching cycle where the minimum and maximum peak loads occur. The effect of pitching motion is most extreme at blade position angles around 135 degrees, where the maximum blade loading occurs. This explains why the time-average loads and the peak loads occur in phase during the pitching cycle.

The unsteady loads are important from consideration of fatigue of the propeller blades, and of the hub mechanism for controllable pitch (CP) propellers. Since a ship may operate for an extended period in a rough sea, the effect of the ship motions, such as hull pitching, on unsteady blade loads is significant. The difference between the peak load and the time-average load per revolution is a measure of the unsteady loading. With this difference as a measure of the unsteady loading, the results with hull pitching showed that the unsteady hydrodynamic loading for the various components increased by 26 to 38 percent above their corresponding values for $\psi = \psi_{CW}$ without hull pitching. This indicates that the effect of ship motions can significantly increase the unsteady loading on the blades.

The difference in the unsteady loading with and without the hull pitching is probably due to an additional relative velocity component arising from the motion of the hull during pitching. As the hull passes through $\psi = \psi_{CW}$ the vertical velocity of the hull (and propeller) is a maximum. As the hull goes from stern-up to stern-down through $\psi = \psi_{CW}$, the upward velocity component relative to the propeller plane tends to increase above the values at fixed hull pitch at $\psi = \psi_{CW}$. This tends to increase the amplitudes of the first harmonic of the tangential velocity, and thereby increase the unsteady loading (and increase the peak loading). The maximum vertical velocity of the propeller for sinusoidal pitching with $(\psi_{MAX} - \psi_{CW}) = 1.33$ degrees and frequency = 0.8 hertz is approximately 0.29 m/s (0.96 ft/s). This is equivalent to additional tangential and radial velocity component ratios (V_t/V and V_r/V, respectively) of 0.082. For ψ fixed at $\psi = \psi_{CW}$, $((V_{t0.7})_1/V) = 0.199$ and $(V_{r0.7})_1/V = 0.145$ (from a harmonic analysis of the wake survey data). Therefore,

$$\frac{(V_{t0.7})_1 + V_\psi}{(V_{t0.7})_1} = \frac{0.199 + 0.082}{0.199} = 1.41$$

and

$$\frac{(V_{r0.7})_1 + V_\psi}{(V_{r0.7})_1} = \frac{0.145 + 0.082}{0.145} = 1.56$$

These maxima occur at $\Theta_\psi = 180$ degrees which essentially agrees with the value of Θ_ψ at which the maximum loads were measured. The measured increase in unsteady loads arising from hull pitching was somewhat smaller than these calculated increases in tangential and radial velocity component ratios, for example:

$$\frac{F_{x_{MAX,\psi}}}{F_{x_{MAX}} - F_x} = \frac{0.89}{0.72} = 1.24$$

Theoretically, the increase in unsteady loading should be approximately proportional to the increases in tangential and radial velocity component ratios; however as shown by Boswell et al. (1981) including calculations in the authors' closure to this paper, the tangential velocity component appears to have a greater influence on periodic blade loads than does the radial velocity component. This simple analysis provides an upper bound to the dynamic pitching load, since the hull boundary above the propeller would tend to reduce the dynamic pitching-induced, upward velocity component relative to the propeller.

Other aspects of the data show the influence of the hull boundary on the upward velocity component relative to the propeller. Figure 13 shows the propeller plane and hull configuration. It is clear that an upward vertical fluid speed relative to the propeller due to pitching would be minimum near the hull centerline corresponding to a blade position angle of 270 degrees. The vertical fluid speed due to pitching would be a maximum at a blade position angle of 90 degrees where it is close to the edge of the hull. Also, some outward turning of the flow would be expected in this region as the hull moves downward into the fluid.

This general character of the flow is represented qualitatively in the effect of pitching on the blade load variation with angular position, shown in Figure 12. As discussed earlier, the effect of pitching is greatest at the outboard blade positions around 100 degrees, where the vertical velocity component due to pitching is greatest. At the inboard positions around 270 degrees, the blade loading is little affected by the pitching motion since the hull boundary restricts the relative vertical velocity. Also shown is a phase shift in the peak

loading between 90 and 135 degrees (also see Figure 11), which may be related to the outward turning of the vertical velocity due to the hull.

Table 3 compares the results presented here for hull pitching in calm water with the same type of results presented by Boswell et al. (1976a, 1976b) for a single-screw transom-stern configuration, and with results presented by Boswell et al. (1978) and Jessup et al. (1977) for a twin-screw transom-stern configuration. The results presented in Table 3 indicate that the experimental results on these three configurations are consistent. The unsteady loads presented in this paper increased by smaller fractions of their values without hull pitching than did the unsteady loads reported by Boswell et al. (1976a, 1976b, 1978); however, this results from the smaller fractional increase in the vertical velocity component relative to the propeller with hull pitching of the present model than with the models reported by Boswell et al. (1976a, 1976b, 1978). The estimated increase in vertical velocity component due to hull pitching was larger than the measured increase in unsteady loading with hull pitching for all three configurations.

Hull pitching was the only one of the six components of ship motions (surge, heave, sway, roll, pitch and yaw) for which blade loads were measured. These experiments showed that hull pitching affects primarily the peak and unsteady blade loading and that this effect appears to be controlled by the ratio of the maximum vertical velocity of the propeller to the ship speed. It appears that the increases in the peak and unsteady blade loading due to the vertical velocity component of the propeller are independent of the type of ship motions producing this vertical velocity. Heave and roll (for propellers off the ship centerline) also produce velocities in the vertical plane of the propeller. Therefore, the effect of heave and roll on the peak and unsteady blade loading can be deduced from the experimental results with hull pitching by calculating the equivalent hull pitching required to produce the same vertical velocity component of the propeller as produced by the specified heave and/or roll.

Surge, sway, and yaw do not significantly alter the flow relative to the propeller in the vertical plane, therefore it is expected that these ship motions would have an insignificant influence on the peak or unsteady blade loading. The primary cause of this unsteady blade load in calm water without ship motions for hulls of the type under consideration here is the upward vertical wake velocity component relative to the propeller plane, therefore any transverse velocity which is small relative to this vertical wake velocity is insignificant when vectorially added to the vertical wake velocity component.

Blade loads were measured for only one pitching frequency. However, any realistic hull pitching frequency is small relative to the propeller rotational frequency; therefore, pitching frequency should not significantly alter the trends of the experimental data. The magnitude of the maximum vertical velocity for a given pitch amplitude is directly proportional to pitching frequency; therefore the peak and unsteady components of blade loading tend to increase as the pitching frequency increases.

Blade loads were measured for only one amplitude of pitching. However, the maximum speed due to pitching is directly proportional to pitching amplitude for a given frequency; therefore, the peak and unsteady blade loading tends to increase as the amplitude of pitching increases. At large amplitudes of pitch the propeller may draw air near the stern-up position. This would tend to unload the blade in the upper portion of the propeller disk so that the unsteady blade loads would increase but the peak loads would not increase. However, this is not the portion of the pitch cycle at which the maximum vertical velocity of the propeller occurs, therefore it appears that maximum steady loads would be controlled by the maximum vertical velocity of the propeller rather than by the air drawing.

Based on these results and those presented by Boswell et al. (1976a, 1976b, 1978), the increase in blade loads due to hull pitching can be estimated for transom stern configurations as follows:

1. Time-Average Loads Per Propeller Revolution

Hull pitching increases the maximum time-average loads per revolution by only a small amount over the time-average loads per revolution without hull pitching. This increase can be approximated as follows:

$$\Delta\overline{L}_{MAX,\psi} \approx (\overline{L})(2\psi_A) \simeq (\overline{L}_\psi)(\psi_A)$$

where $\Delta\overline{L}_{MAX,\psi}$ = maximum increase in time-average loads per revolution with hull pitching over the value in calm water

$\overline{L}$ = time-average load in calm water

$\overline{L}_\psi$ = time-average load in waves

ψ_A = amplitude of the variation in hull pitch angle in radians

In practice, this maximum increase in time-average loads per revolution due to pitching is negligible relative to the corresponding increase due to waves, as discussed later.

2. Periodic Loads

Hull pitching (in calm water) substantially increases the maximum periodic blade loads over the corresponding periodic loads without hull pitching. The primary controlling parameter is the ratio of the vertical velocity of the propeller resulting from the hull pitching to the ship speed. The maximum periodic loads occur when the velocity of the propeller and stern are maximum downward. This downward velocity of the propeller effectively increases the inclination of the inflow relative to the propeller and thereby increases the periodic load. Due to the

displacement effect of the hull above the propeller, the vertical speed of the propeller relative to the local fluid particles is only 60 percent or less of the vertical speed of the propeller. Therefore, for ships with high-speed transom sterns with exposed shafts and struts, the maximum periodic blade loads due to hull pitching can be approximated from the corresponding loads without hull pitching as follows:

$$\Delta\tilde{L}_{MAX,\psi} \approx \frac{0.6\ V_{\psi}}{V_C}\ \tilde{L}$$

where $\Delta\tilde{L}_{MAX,\psi}$ = maximum increase in periodic loads with hull pitching over the values without ship motions

$\tilde{L}$ = periodic blade load without ship motions

V_C = vertical component of spatial average crossflow velocity in propeller plane without ship motions

V_{ψ} = maximum vertical velocity component of the propeller due to the pitching motions

3. Peak Loads

The maximum values of the periodic variation of loads with angular position and the time-average loads per angular position occur near the same point in the pitch cycle. Therefore, the increase in peak loads due to hull pitching is approximately the sum of the increases in these components:

$$\Delta L_{PEAK,\psi} \approx \Delta\bar{L}_{MAX,\psi} + \Delta\tilde{L}_{MAX,\psi}$$

The nZ-1, nZ, and nZ+1 harmonics of blade loads directly contribute to the periodic loads on the propeller shaft and bearings. Full scale measurements (Tasaki, 1975) indicate that the amplitudes of periodic bearing loads are modulated by the influences of a rough sea. The maximum amplitudes of these modulated loads at blade rate frequency are commonly more than a factor of two greater than the corresponding amplitudes of the loads measured in a calm sea as discussed by Lipis (1975) and Tasaki (1975). In the present investigation, the influence of hull pitching on periodic bearing loads was investigated by evaluating the influence of pitching on the pertinent harmonics of blade loads.

In the investigations described by Boswell et al. (1976a, 1976b, 1978), no analysis was made of the harmonics of blade loads beyond the dominant first harmonic because of their small amplitudes which were, in many cases, around one percent of the time-average thrust (for forces) and torque (for moments). However, for evaluating the effects of waves and pitching on periodic bearing loads, the variations of these

quantities with wave and pitching parameters are more important than the actual values of the small, pertinent higher harmonics of blade loads.

Figure 14 shows the variations of the first 10 harmonics of the F_x component of blade loading with location through one pitch cycle. The value of each harmonic amplitude is nondimensionalized on its calm water value. The variations of the amplitudes of the second, third and fourth harmonic are similar in magnitude to the dominant first harmonic of blade loading. These components are the major contributors to the blade loading variation with blade angle, as shown in Figure 9. The amplitudes of the fifth through the eighth harmonics show much larger variations with pitch angle relative to the respective time-average values. This result implies that the relatively small, higher harmonics of blade loading associated with unsteady bearing forces, are very sensitive to relatively small changes in the wake pattern.

F. Operation in Waves Without Hull Pitching

Figure 15 presents the variations of the peak values per revolution, time-average values per revolution, and the first harmonic values of the F_x and M_x components of hydrodynamic blade loading with wave height for operation in waves without hull pitching (Condition 3 in Table 1). The F_y and M_y components showed similar variations as in Figure 15, and the F_z and M_z components were found to be relatively independent of wave height. Table 5 summarizes the maximum absolute values of the peak loads, first harmonic loads, and time-average loads per revolution for operation in waves without hull pitching.

The maximum absolute values of the time-average loads per revolution $\bar{L}_{MAX,\zeta}$ increased by as much as 14 percent above the corresponding time-average loads in calm water without hull pitching $\bar{L}_{MAX}$. This is quite different from the corresponding result with hull pitching in calm water where the time-average loads per revolution increased by a maximum of only 5 percent above the corresponding time-average loads in calm water without hull pitching. The variations of the time-average loads per revolution approximately followed the local wave elevation in the propeller plane so that the maximum and minimum time-average loads per revolution occurred at approximately 36 degrees of the wave cycle of encounter before the time at which the wave trough and peak, respectively, were in the propeller plane.

The variations of the time-average loads per revolution with position in the wave are consistent with trends reported by McCarthy et al. (1961). McCarthy et al. measured the low frequency variation of propeller shaft thrust and torque with position in the wave for steady ahead operation in regular head waves without ship motions and without a nearby hull. They did not measure individual blade loads; however, the variations of low frequency shaft thrust and torque are essentially the same as the variations of the time-average values per revolution of blade thrust $\bar{F}_x$ and blade torque $\bar{M}_x$. The results of McCarthy et al. agreed with the results of the present investigation in that the maximum values of the thrust coefficient $\bar{K}_T$ and torque coefficient $\bar{K}_Q$

occurred when the trough of the wave was near the propeller plane, and the minimum values of $\overline{K}_T$ and $\overline{K}_Q$ occurred when the crest of the wave was near the propeller plane.

The variations of the time-average loads per revolution are also reasonably consistent with trends predicted by a combination of trochoidal wave theory and the quasi-steady propeller theory of McCarthy (1961). According to trochoidal wave theory, the orbital velocities in the head waves vectorially combine with the propeller speed of advance so that speed into the propeller is a maximum when the crest of the wave is in the propeller plane, and the axial velocity component into the propeller is a minimum when the trough of the wave is in the propeller plane. According to simple quasi-steady propeller theory, which should be valid for the low frequency variation of the velocity components in a wave, the maximum and minimum time-average loads per revolution occur when the speed into the propeller plane is minimum and maximum, respectively.

The maximum absolute values in waves of time-average thrust per blade $\overline{F}_{x_{H,MAX,\zeta}}$ and time-average torque per blade $\overline{M}_{x_{H,MAX,\zeta}}$, were compared with values caluclated by trochoidal wave theory and quasi-steady propeller theory. In these calculations, the spatial average velocity through the propeller disk under the trough of a trochoidal wave was determined using the formulation of McCarthy et al. (1961). This formulation does not consider any possible effect of the hull on trochoidal wave velocities. This spatial average velocity and the quasi-steady procedures of McCarthy (1961) were used to calculate the values of $\overline{F}_{x_{H,MAX,\zeta}}$ and $\overline{M}_{x_{H,MAX,\zeta}}$. The comparison with experimental results is as follows:

	Experimental	Theoretical
$\overline{F}_{x_{H,MAX,\zeta}}/\overline{F}_{x_H}$	1.12	1.14
$\overline{M}_{x_{H,MAX,\zeta}}$	1.09	1.11

This agreement between theory and experiment is considered to be satisfactory and correlates well with the findings of McCarthy et al. (1961) and others as summarized by Tasaki (1975). The small differences between theory and experiment may be due to the influence of the hull on wave velocity distribution. The effect of the hull may account for the discrepancy between theory and experiment of the relative phase between the maximum mean loads and the wave trough. The measured result showed the phase of the maximum load leads the theoretical result by approximately one-eighth of the wavelength.

The maximum absolute values of the peak minus time-average loads per revolution $\tilde{L}_{MAX,\zeta}$ increased by as much as 12 percent of the time-average loads in calm water without hull pitching above the corresponding peak minus time-average loads in calm water without hull pitching, $L_{MAX}-\overline{L}$ (see Table 4). Similarly, the maximum values of the first

harmonic loads $(L)_{1MAX}$, increased as much as 9 percent of the time-average loads in calm water without hull pitching above the corresponding first harmonic loads in calm water without hull pitching, $(L)_1$. The variations of the peak minus time-average loads per revolution and the first harmonic loads approximately followed the local wave elevation in the propeller plane so that their maximum absolute values occurred at approximately 45 degrees of the cycle of encounter before the time at which local wave elevation passes through the calm water level from negative to positive ($\zeta = 0$, $\dot{\zeta}>0$).

The variations of the peak minus time-average loads per revolution and first harmonic loads are reasonably consistent with trends predicted by trochoidal wave theory. According to computations by McCarthy et al. (1961) using trochoidal wave theory, the longitudinal components of the orbital velocities are essentially independent of location in the propeller disk; therefore, the longitudinal components of orbital velocities do not contribute to the circumferential variations of propeller blade loads. Trochoidal wave theory predicts that the vertical components of the orbital velocities in the head waves reach their maximum values in the upward direction at the position where $\zeta = 0$ and $\dot{\zeta}>0$. The wake into the propeller disk for the present hull is predominantly an upward velocity due to the inclination of the propeller shaft relative to the hull (see Figure 6); therefore, at $\zeta = 0$, $\dot{\zeta}>0$ the orbital velocity and the wake velocity vectorially combine to produce the maximum upward velocity relative to the propeller, which is equivalent to the maximum first harmonic of the tangential velocity. The first harmonic of the tangential wake is the primary cause of the unsteady blade loads on the present hull operating in calm water without pitching; therefore, the maximum unsteady loads in trochoidal waves should occur at $\zeta = 0$, $\dot{\zeta}>0$. The measured results show the phase of the maximum unsteady loads leads the predicted result by approximately one-eighth of a wavelength.

The ratio of the maximum variation of blade loading with blade angular position in waves to the corresponding variation of blade loading in calm water should be proportional to the ratio of the maximum vertical velocity in waves to the corresponding vertical velocity in calm water (since the vertical velocity is proportional to the first harmonic of the tangential component of velocity). The temporal maximum upward vertical velocity in the propeller plane (this velocity is essentially constant over the propeller disk) in a trochoidal wave corresponding to Condition 3 in Table 1 was calculated using the formulation of McCarthy et al. (1961) to be 0.235 m/s (0.772 ft/s). This is equivalent to an additional tangential velocity ratio V_t/V of 0.066. The value of $(V_{t0.7})_1/V$ for operation in calm water is 0.199 from the wake survey results. Therefore,

$$\frac{(V_{t0.7})_{1MAX}/V}{(V_{t0.7})_1/V} = \frac{0.199 + 0.066}{0.199} = 1.33$$

This maximum ratio, which does not consider the effect of the hull on the vertical component of the trochoidal wave velocities, is predicted to occur when the wave elevation at the propeller plane is increasing through the calm water level, i.e., $\zeta = 0$, $\dot{\zeta}>0$. The measured increase in the variation of loads with blade angular position for operation in waves was somewhat smaller than this calculated increase in tangential velocity; for example:

$$\tilde{F}_{x_{MAX,\zeta}} / (F_{x_{MAX}} - \overline{F}) = 1.17$$

$$(F_x)_{1MAX,\zeta} / (F_x)_1 = 1.12$$

This simple analysis is believed to provide an upper bound to the increase in variation of loads with blade angular position due to operation in waves, since the hull boundary above the propeller would tend to reduce the vertical component of the trochoidal wave velocity. The corresponding measured increase for other components of blade loading are presented in Table 5.

The maximum absolute values of the peak loads per revolution increased by as much as 22 percent of the time-average loads in calm water without hull pitching above the corresponding peak loads in calm water without hull pitching (see Table 5). This increase in peak loads is made up of the increase in the time-average loads per revolution (up to 14 percent) and the increase in the circumferential variation in loads, or peak minus time-average loads per revolution (up to 12 percent). The increases in the time-average loads per revolution and the increases in circumferential variations of loads are thought to arise from different physical characteristics of the flow as discussed previously; however, the maximum increase in the time-average loads and circumferential variations of loads occur in the same portion of the wave period. Therefore, these two separate increases tend to add almost in phase relative to the wave period so that the maximum increase in peak loads is almost the algebraic sum of the maximum increases in the time-average loads per revolution and the maximum increase in the circumferential variation of loads.

Figure 16 shows the variation of the F_x component of blade load with angular position for different times during one wave cycle. The variation of the circumferential distribution to waves appears to be more complicated than the corresponding variation due to pitching. This is attributed to the combined effect of the longitudinal and vertical velocities induced by the wave. As in the case of pitching, the greatest magnitude of loading occurs at blade angles around 90 degrees, corresponding to the outboard position of the blades relative to the propeller shaft. Also, the phase angle of the maximum load varies with position relative to the wave, but with the combined effects of mean and unsteady load variations no clear trends are observed. The variation

in first harmonic phase shown in Figure 15 indicates a significant change in vertical flow direction due to the hull.

Blade loads were measured in regular head waves at only one wave amplitude and wavelength. The experiments showed that the increases in both the time-average loads per revolution and the unsteady loads due to waves appears to be controlled by the orbital velocity in a trochoidal wave. It appears that the increase in both the time-average loads per revolution and the unsteady loads are proportional to the orbital velocity. The orbital velocity, and thus the approximate increase in loads, is directly proportional to the wave height and inversely proportional to the square root of the wavelength (Lewis, 1967, McCarthy et al., 1961), neglecting any possible influence of the hull on these trends.

The vertical component of the orbital velocity, which controls the increase in unsteady blade loading due to waves, is independent of the direction of the waves relative to the ship heading. Therefore, the increase in unsteady blade loading due to waves is essentially independent of the relative direction of the waves. The component of the orbital velocity in the direction of the ship velocity, which controls the increase in the time-average loads per revolution due to waves, is proportional to the cosine of μ, the angle between the direction of the waves and the ship heading. Therefore, the increase in the time-average loads per revolution is essentially proportional to cos μ, neglecting any possible influence of the hull on these trends.

Based on these results the increases in blade loads due to waves can be estimated for transom-stern configurations as follows:

1. Time-Average Loads Per Revolution

Waves (without ship motions) substantially increase the maximum time-average loads per revolution over the corresponding time-average loads in calm water. The primary controlling parameter is the change in effective advance coefficient due to the longitudinal component of orbital wave velocity. The hull boundary above the propeller does not appear to significantly influence the longitudinal component of orbital wave velocity. Therefore, the maximum increase in time-average loads per propeller revolution due to waves can be adequately predicted by the use of the trochoidal wave theory neglecting the influence of the hull on the waves, and simple quasi-steady propeller theory using the open-water characteristics of the propeller.

2. Periodic Loads

Waves (without ship motions) substantially increase the maximum periodic blade loads over the corresponding periodic loads in calm water. The primary controlling parameter is the ratio of the vertical component of the orbital wave velocity in the propeller plane to the ship speed. The maximum periodic loads occur when the vertical component of the orbital wave velocity in the propeller plane is maximum upward. This upward orbital velocity component effectively increases the inclination of the inflow to the propeller and thereby increases

the periodic loads. Due to the hull boundary above the propeller, the maximum upward orbital velocity into the propeller is only 50 percent or less of the corresponding upward orbital velocity in an unbounded fluid for ships with high-speed transom sterns and exposed shafts and struts. Therefore, for these ships the maximum periodic blade loads due to waves can be approximated from the corresponding loads without waves as follows:

$$\Delta\tilde{L}_{MAX,\zeta} \approx \frac{0.5\ V_\zeta}{(V_{t0.7})_1}\tilde{L} \simeq \frac{0.5\ V_\zeta}{V_C}\tilde{L}$$

where $\Delta\tilde{L}_{MAX,\zeta}$ = maximum increase in periodic loads with waves over the values in calm water

$\tilde{L}$ = periodic blade load in calm water

V_ζ = maximum vertical component of the orbital wave velocity in the propeller plane neglecting the influence of the hull

$(V_{t0.7})_1$ = first harmonic of the tangential wake at the 0.7 radius in calm water

V_C = vertical component of spatial average crossflow velocity in propeller plane in calm water

3. Peak Loads

The maximum values of the periodic variation of loads with angular position and the time-average loads per angular position occur near the same point in the wave cycle. Therefore, the increase in peak loads due to waves is approximately the sum of the increases in these components:

$$\Delta L_{PEAK,\zeta} \approx \Delta\bar{L}_{MAX,\zeta} + \Delta\tilde{L}_{MAX,\zeta}$$

Figure 17 shows the variations of the higher harmonic amplitudes of the F_x component of blade load through the wave height cycle. For the case of waves, it appears that the second through fifth harmonic amplitudes show distinct periodic variations up to 50 percent of the calm water values. The sixth through tenth harmonic amplitudes show a more random variation of a lesser extent. This is contrary to the pitching results where less variation occurred over the greater and lesser harmonics and extreme variations occurred in the fifth through eighth harmonics. The large variation in the third, fourth, and fifth harmonic amplitudes of F_x would lead to significant modulation in the periodic bearing forces produced by the four-bladed model propeller. The large variation in the second through fourth harmonic amplitudes

of F_x, the amplitudes of which range from 2 to 13 percent of the time-average value, also explain some of the complexity of the wave forms shown in Figure 16. These harmonics have consistent variations in phase angles of up to 45 degrees.

G. Operation in Waves With Hull Pitching

As discussed in the section on experimental conditions and procedures, for forced pitching in waves the phase of the wave at the propeller Φ_ζ was varied relative to the phase of the hull pitching Φ_ψ. Three relative phases were evaluated:

a. Wave crest at the propeller plane when the stern of the model hull is pitched up at its maximum value, $\Phi_\zeta - \Phi_\psi = 0$ (Condition 4 in Table 1),

b. Wave crest at the propeller plane when the stern of the model hull is pitched down at its maximum values, $\Phi_\zeta - \Phi_\psi = 180$ degrees (Condition 5 in Table 1), and

c. Wave crest at the propeller plane when the hull pitch is passing through its mean value $(\psi_{MAX} - \psi_{MIN})/2$ from stern down to stern up, $\Phi_\zeta - \Phi_\psi = 90$ degrees (Condition 6 in Table 1).

Experiments for each of these conditions were conducted at the same model speed, propeller rotation speed, pitching period, wave period of encounter as were the condition in calm water with hull pitching, and in waves without hull pitching, as described in the preceding sections (see Table 1). However, in order to ensure a large influence of the pitching or waves on blade loads while not flooding the model hull, it was necessary to run each of the four pitching conditions with a different pitch amplitude ψ_A, and each of the four conditions in waves with a different wave amplitude ζ_A (see Table 1).

The primary objectives of this portion of the experimental program were:

a. To determine the validity of linearly superimposing the increase in blade loads due to pitching in calm water, and the increase in blade loads due to waves without hull pitching, to obtain the net increase in blade loads due to hull pitching in waves,

b. To determine the influence of the phase of the hull pitch relative to the phase of the wave $(\Phi_\zeta - \Phi_\psi)$ on the maximum absolute values of the peak, unsteady and time-average blade loads, and

c. To determine the values of $(\Phi_\zeta - \Phi_\psi)$ which result in the largest values of peak, unsteady and time-average blade loads for different relative values of pitching amplitude ψ_A and nondimensional wave amplitude, ζ_A/L_{PP}.

Therefore, the experimental results will be discussed and interpreted from the viewpoint of these three objectives.

In order to determine the validity of linearly superimposing the increase in blade loads due to the pitching only and the increase in blade loads due to waves only, the experimental results with hull pitching in calm water and the experimental results in waves without hull pitching were linearly combined to simulate the blade loads for the

three experimental conditions with hull pitching in waves. The linear superposition accounts for the phase differences between the hull pitching and the waves, and for the differences in amplitudes of pitching and waves for the various experimental conditions. It is assumed in this linear superposition that the increases in loading due to hull pitching and waves are directly proportional to the amplitude of the hull pitching and the amplitude of the waves, respectively.

From the experiments in calm water with hull pitching (Condition 2 in Table 1) the increase in loading due to a unit pitch amplitude is:

$$\Delta\bar{L}_{\psi}(t_{\psi})/\psi_A = (L_{\psi}(t_{\psi}) - \bar{L})/\psi_A$$

$$\Delta\tilde{L}_{\psi}(t_{\psi})/\psi_A = (\tilde{L}_{\psi}(t_{\psi}) - (L_{MAX} - \bar{L}))/\psi_A$$

From the experiments in waves without hull pitching (Condition 3 in Table 1) the increase in loading due to a unit wave amplitude is:

$$\Delta\bar{L}_{\zeta}(t_{\zeta})/\zeta_A = (L_{\zeta}(t_{\zeta}) - \bar{L})/\zeta_A$$

$$\Delta\tilde{L}_{\zeta}(t_{\zeta})/\zeta_A = (\tilde{L}_{\zeta}(t_{\zeta}) - (L_{MAX} - \bar{L}))/\zeta_A$$

Linearly superimposing the above increases in loading due to pitching only and due to waves only, the predicted loads with pitching amplitude ψ_A^*, wave amplitude ζ_A^*, and with the wave leading the pitch by $(\Phi_{\zeta} - \Phi_{\psi})T_E/2\pi$ seconds is

$$\bar{L}_{\psi,\zeta}(t_{\psi}) = \Delta\bar{L}_{\psi}(t_{\psi})\psi_A^* + \Delta\bar{L}_{\zeta}((t_{\zeta} + (\Phi_{\zeta} - \Phi_{\psi})T_E/2\pi)\zeta_A^* + \bar{L}$$

$$\tilde{L}_{\psi,\zeta}(t_{\psi}) = \Delta\tilde{L}_{\psi}(t_{\psi})\psi_A^* + \Delta\tilde{L}_{\zeta}((t_{\zeta} + (\Phi_{\zeta} - \Phi_{\psi})T_E/2\pi)\zeta_A^* + (L_{MAX} - \bar{L})$$

$$L_{PEAK,\psi,\zeta}(t_{\psi}) = \bar{L}_{\psi,\zeta} + \tilde{L}_{\psi,\zeta}(t_{\psi})$$

Figure 18 compares F_X component loads calculated by this linear superposition procedure with loads measured in waves with hull pitching for the three conditions run, $\Phi_{\zeta} - \Phi_{\psi} = 0$, $\Phi_{\zeta} - \Phi_{\psi} = 180$, $\Phi_{\zeta} - \Phi_{\psi} = 90$ degrees. Figure 18 shows that the linear superposition gives a reasonably good estimate of both the magnitudes and the variations with position in the pitch and wave cycles of the peak loads, unsteady loads, and time-average loads per revolution. For most conditions the values based on linear superposition are slightly larger than the measured results.

Therefore, it is concluded that linear superposition of the separate increases in blade loads due to pitching and waves gives a good, or slightly conservative, estimate of net increase in blade loads due to operation in waves with hull pitching.

In order to evaluate the relative importance of the amplitude of hull pitching, the amplitude of the waves, and the phase difference between the hull pitch and the wave at the propeller, the experimental results with hull pitching in calm water and the experimental results in waves without hull pitching are linearly combined as described previously to simulate blade loads for the following values of ψ_A, and ζ_A/L_{PP}:

ψ_A = 1.0 degrees, ζ_A/L_{PP} = 0.01 - representing calm to moderate sea conditions

ψ_A = 2.0 degrees, ζ_A/L_{PP} = 0.03 - representing moderate to rough sea conditions

Figure 19 presents the maximum values of the F_x component time-average loads per revolution, peak loads per revolution, and the peak minus time-average loads per revolution calculated by linear superposition for the selected values of pitch amplitude and wave amplitude over the complete range of the relative phase between the pitch and the wave. Only the F_x component is shown since the pertinent trends are basically the same for the F_x, M_y, M_x, and F_y components. The abscissa of these curves, $\Phi_\zeta - \Phi_\psi$, is the phase angle by which the pitch lags the wave at the propeller relative to the frequency of encounter or the pitching frequency.

The results shown in Figure 19 indicate that for given amplitudes of waves and pitching the maximum values of the time-average loads per revolution, peak loads, and unsteady loads (peak loads minus time-average loads per revolution) vary substantially depending on the difference in phase between the hull pitch and the wave at the propeller, $\Phi_\zeta - \Phi_\psi$. The peak loads are more sensitive to this difference in phase than are the unsteady loads which, in turn, are more sensitive than the time-average loads per revolution. The time-average loads, peak loads, and periodic loads are near their respective largest values in the region where $-30 \text{ degrees} < (\Phi_\zeta - \Phi_\psi) < 120 \text{ degrees}$; i.e., where the crest of wave reaches the propeller between 120 degrees before and 30 degrees after the maximum stern-up position in the pitch cycle. Over this region of $\Phi_\zeta - \Phi_\psi$ the maximum increase in loads due to pitching in calm water and the maximum increase in loads due to waves without hull pitching add almost algebraically, i.e., there is very little cancellation due to phase differences between these increases. The values of the maximum peak loads and maximum unsteady loads reach their smallest values near $\Phi_\zeta - \Phi_\psi = 240$ degrees. These trends hold true for the F_x, M_y, F_y and M_x components for all combinations of amplitudes of hull pitching and amplitude of waves which were evaluated.

In summary, the experiments with hull pitching in regular head waves with pitching frequency equal to the wave frequency of encounter showed the following:

a. For given amplitudes of waves and pitching the maximum values of the time-average loads per revolution, peak loads, and the periodic variation of loads with angular position vary substantially depending upon the difference in phase between the hull pitch and the wave at the propeller. The time-average loads, peak loads, and periodic loads are near their respective greatest values for any difference in phase whereby the crest of the wave reaches the propeller between 0.3 and -0.1 of the period of encounter before the maximum stern-up position.

b. Linear superposition of the increases in blade loads due to pitching in calm water and due to waves without hull pitching, taking into account the phase between the waves and the pitching, gives a satisfactory, or slightly conservative, estimate of the net increase in blade loads due to operation in waves with hull pitching. For engineering calculations, it is recommended that the absolute values of the maximum increases in time-average, peak, and periodic loads due to the separate influences of waves and hull pitching be added without regard to the relative phase between the wave and the hull pitching.

IV. DISCUSSION

The results presented in this paper showing the effects of hull pitching and waves on the dominant once per propeller revolution variation of loads provide extensive insight to the flow patterns in the propeller plane under these conditions. These data and insights should form a basis for developing and validating a computational procedure for predicting blade loads under these conditions.

The experimental results presented here are applicable to only high speed transom stern configurations. The influences of the hull boundary of more complex stern geometries, such as for full stern cargo ships, are more complex. Experiments of the type described in this paper would serve as a valuable guide for validating any computational procedure applied to cargo ships.

The prediction of the modulation of bearing loads due to waves and pitching cannot be performed using the simple procedures described in this paper. More elaborate models of the interaction between the propeller wake and the waves and pitching influences may capture the fundamental nature of the modulation of the bearing loads.

All results presented in this paper are in the absence of cavitation. It is anticipated that if cavitation were sufficiently extensive to influence blade loads it would reduce the maximum time-average and periodic loads. Therefore, it is judged that neglecting cavitation results in a conservative estimate of maximum loads.

V. SUMMARY AND CONCLUSIONS

Fundamental investigations were made of the effects of periodic hull pitching motions and waves on the periodic loads on propeller blades and bearings. These periodic loads were measured during carefully controlled model experiments on a twin-screw, transom-stern hull. The objective of these experiments was to obtain systematic accurate experimental data showing the effects of hull pitching and waves on periodic and time-average blade and bearing loads under carefully controlled experimental conditions so that the effects of ship motions and waves on periodic and time-average blade and bearing loads could be isolated. The experiments were conducted under steady ahead operation in calm water with no ship motions, in calm water with forced sinusoidal pitching of the hull, in regular waves with no ship motions, and in regular waves with forced sinusoidal pitching of the hull at a frequency equal to the wave frequency of encounter over a range of phases between the pitching motion and wave encounter. An error analysis indicates that the experimental results are sufficiently accurate to support the conclusions drawn. The periodic blade loads were calculated using trochoidal wave velocity profiles, and a representation of the propeller based on a quasi-steady method.

The experimental results show the following:

a. The amplitudes of the periodic blade loads are significantly modulated hull pitching motions and wave encounter.

b. The time-average blade loads per propeller revolution vary significantly with wave encounter but only slightly with hull pitching motion.

c. The peak blade loads per revolution vary significantly with hull pitching motions and wave encounter.

d. The individual influences of the wave velocity profile and the induced velocities due to vertical hull motions can be linearly superimposed for transom stern configurations.

The results show that the hull significantly alters the amount of modulation of the shaft frequency loads due to both the periodic vertical motion of the propeller and the trochoidal wave velocity profile in the absence of the hull. However, trends of shaft frequency loads are well predicted by simple periodic variations of the velocity into the propeller, and a simple quasi-steady representation of the propeller. The quasi-steady representation of the propeller is sufficient for this application because the frequencies of encounter of the waves and of the hull pitching motions are low relative to the propeller rotational speed; i.e., the reduced frequency is low. Therefore, for engineering purposes, the modulation can be estimated by simple trochoidal wave velocity profiles, quasi-steady propeller theory, and constant multiples derived from the experiments presented in this paper.

The experimental results show that the first eight shaft rate harmonics of blade loads are modulated and increased by hull pitching motions and waves relative to the respective values in calm water without hull pitching. Comparable modulations and increases in bearing loads

are anticipated, where the number of blades determines the pertinent harmonics of blade loading. However, the data are not sufficient to quantify the modulations of bearing loads due to hull pitching and waves nor to provide guidance for predicting these modulations.

Trends of the results for both blade loads and bearing loads are consistent with available full-scale data.

VI. ACKNOWLEDGMENTS

The authors are indebted to many members of the staff of the David W. Taylor Naval Ship Research and Development Center. Special appreciation is extended to Messrs. Michael Jeffers, Benjamin Wisler, and Douglas Dahmer for development of the on-line data analysis sytem, assembling the servomechanism for accurately controlling the model pitching relative to the waves, assisting in running the experiments, and analyzing data.

VII. REFERENCES

Boswell, R. J., and M. L. Miller (1968). Unsteady Propeller Loading - Measurement, Correlation with Theory, and Parametric Study, NSRDC Rept 2625.

Boswell, R. J., J. J. Nelka, and S. B. Denny (1976). Experimental Determination of Mean and Unsteady Loads on a Model CP Propeller Blade for Various Simulated Modes of Ship Operation, Eleventh Symposium on Naval Hydrodynamics, Mechanical Engineering Publications Limited, London and New York, pp. 789-834.

Boswell, R. J., J. J. Nelka, and S. B. Denny (1976). Experimental Unsteady and Mean Loads on a CP Propeller Blade on the FF-1088 for Simulated Modes of Operation, DTNSRDC Rept 76-0125, DTIC ADA 034804.

Boswell, R. J., S. D. Jessup, and J. J. Nelka (1978). Experimental Time Average and Unsteady Loads on the Blades of a CP Propeller Behind a Model of the DD-963 Class Destroyer, Propellers '78 Symposium, The Society of Naval Architects and Marine Engineers Publication S-6, pp. 7/1-7/28.

Boswell, R. J., S. D. Jessup, and K. H. Kim (1981). Periodic Blade Loads on Propellers in Tangential and Longitudinal Wakes, Propellers '81 Symposium, The Society of Naval Architects and Marine Engineers Publication S-8, also DTNSRDC Rept 81/054.

Brandau, J. H. (1968). Static and Dynamic Calibration of Propeller Model Fluctuating Force Balances, DTMB Rept 2350, also Technologia Naval, 1, pp. 48-74.

Breslin, J. P. (1972). Propeller Excitation Theory, Proc. 13th International Towing Tank Conference, Report of the Propeller Committee, App. 2c, 2, pp. 527-540.

Brownell, W. F., W. L. Asling, and W. Marks (1956). A 51-Foot Pneumatic Wave-maker and a Wave Absorber, DTMB Rept 1054.

Day, W. G., A. M. Reed, and W.-C. Lin (1977). Experimental and Prediction Techniques for Estimating Added Power Requirements in a Seaway, Proc. 18th American Towing Tank Conference, U.S. Naval Academy, Annapolis, Maryland, I, pp. 121-141.

Dobay, G. F. (1971). Time-Dependent Blade-Load Measurements on a Screw-Propeller, Presented at the 16th American Towing Tank Conference, Instituto De Pesquisas Technologicas, Marinhas Do Brasil.

Gray, L. M. (1981). Investigation into Modeling and Measurement of Propeller Cavitation Source Strength at Blade Rate on Merchant Vessels, Propellers '81 Symposium, The Society of Naval Architects and Marine Engineers Publication S-8, pp. 165-180.

Jessup, S. D., R. J. Boswell, and J. J. Nelka (1977). Experimental Unsteady and Time Average Loads on the Blades of the CP Propeller on a Model of the DD-963 Class Destroyer for Simulated Modes of Operation, DTNSRDC Rept 77-0110, DTIC ADA-048385.

Keil, H. G, J. J. Blaurock, and E. A. Weitendorf (1972). Stresses in the Blades of a Cargo Ship Propeller, J. of Hydronautics, 6, 1, pp. 2-7.

Lewis, E. V. (1967). Motion of Ships in Waves, Chapter IX, Principles of Naval Architecture, Edited by J. P. Comstock, The Society of Naval Architects and Marine Engineers, pp. 607-717.

Lipis, B. V. (1975). Hydrodynamics of a Screw Propeller with Motions of the Vessel (in Russian: Gidrodinamika Grebnogo Vinta pri Kachke Sudna), Publishing House Sudostroyeniye, Leningrad.

Lloyd, A. R. J. M., and R. N. Andrew (1977). Criteria of Ship Speed in Rough Weather, Proc. 18th American Towing Tank Conference, U.S. Naval Academy, Annapolis, Maryland, II, pp. 541-564.

McCarthy, J. H. (1961). On the Calculation of Thrust and Torque Fluctuations of Propellers in Nonuniform Wake Flow, DTMB Rept 1533.

McCarthy, J. H., W. H. Norley, and G. L. Ober (1961). The Performance of a Fully Submerged Propeller in Regular Waves, DTMB Rept 1440.

Oosterveld, M. W. C. (editor) (1978). Report of the Seakeeping Committee, 15th International Towing Tank Conference, The Netherlands Ship Model Basin, Wageningen, pp. 55-114.

Schwanecke, H. (1975). Comparative Calculations on Unsteady Propeller Blade Forces, Proc. 14th International Towing Tank Conference, Report of the Propeller Committee, App 4, 3, pp. 357-397.

Tasaki, R. (1975). Propulsion Factors and Fluctuating Propeller Loads in Waves, Proc. 14th International Towing Tank Conference, Report of Seakeeping Committee, App 7, 4, pp. 224-236.

Tsakonas, S., W. R. Jacobs, and M. R. Ali (1974). An Exact Linear Lifting Surface Theory for Marine Propeller in a Nonuniform Flow Field, J. of Ship Research, 17, 4, pp. 196-207.

Watanabe, K., N. Heida, T. Sasajima, and T. Matsuo (1973). Propeller Stress Measurements on the Container Ship HKONE MARU, Shipbuilding Research Association of Japan, 3, 3, pp. 41-51.

NOTATION

c	Chord length
D	Propeller diameter
$(F)_n$	nth harmonic amplitude of F
$F_{x,y,z}$	Force components on blade in x,y,z directions
J_Q	Effective advance coefficient based on torque identity
J_T	Effective advance coefficient based on thrust identity
K_Q	Torque coefficient, $Q/(\rho n^2 D^5)$
K_T	Thrust coefficient, $T/(\rho n^2 D^4)$
L	Any of the measured components of blade loading
L_{PP}	Length between perpendiculars
L_W	Wavelength
$(M)_n$	nth harmonic amplitude of M
$M_{x,y,z}$	Moment components about x,y,z axes from loading on one blade
n	Propeller revolutions per unit time
R	Radius of propeller
r	Radial coordinate from propeller axis
T_E	Period of encounter of waves
T_ψ	Period of pitching
t	Time
$t(r)$	Maximum thickness of propeller blade section
V	Model speed or ship speed
V_A	Propeller speed of advance
V_C	Vertical component of the spatial average crossflow velocity in propeller plane in calm water without ship motions
$V_r(r,\theta_W)$	Radial component of wake velocity at propeller plane, positive towards hub
$V_t(r,\theta_W)$	Tangential component of wake velocity at propeller plane, positive counterclockwise looking upstream for starboard propeller (right-hand rotation), positive clockwise looking upstream for port propeller (left-hand rotation)
$(V_t)_n$	nth harmonic amplitude of V_t
V_W	Wave velocity
$V_x(r,\theta_W)$	Longitudinal component of wake velocity at propeller plane, positive forward
V_ψ	Maximum vertical velocity component of propeller resulting from hull pitching motions
w_Q	Taylor wake fraction determined from torque identity
w_T	Taylor wake fraction determined from thrust identity
w_{VM}	Wake fraction determined from volume mean longitudinal velocity component through propeller disk determined from a wake survey, $(V-V_{VM})/V$
x,y,z	Coordinate axes rotating with propeller; see Figure 2
Z	Number of blades
ζ	Instantaneous wave elevation, positive upward from undisturbed surface
ζ_A	Wave amplitude

Θ_ζ Angular variable in cycle of wave encounter, $2\pi t/T_E$; $\Theta_\zeta = 0$ when $\zeta = 0$, $\dot{\zeta}>0$

Θ_ψ Angular variable in cycle of hull pitching, $2\pi t/T_\psi$; $\Theta_\psi = 0$ when $\psi = 0$, $\dot{\psi}>0$

θ Angular coordinate used to define location of blade and variation of loads measured from vertical upward; positive clockwise looking upstream for starboard propeller (righ-hand rotation), positive counterclockwise looking upstream for port propeller (left-hand rotation), $\theta = -\theta_W$

θ_W Angular coordinate of wake velocity measured from upward vertical; positive counterclockwise looking upstream for starboard propeller (right-hand rotation), positive clockwise looking upstream for port propeller (left-hand rotation), $\theta_W = -\theta$

μ Angle between the direction of the waves and the ship centerline

ρ Mass density of water

Φ_ζ Phase of wave at the propeller plane based on sine series, $\zeta(t) = \zeta_A \sin(\Theta_\zeta + \Phi_\zeta)$

Φ_ψ Phase of hull pitch based on sine series, $\psi(t) = \psi_A \sin(\Theta_\psi + \Phi_\psi)$

$\phi(r)$ Pitch angle of propeller blade section, $\tan^{-1}(P/(2\pi r))$

$(\phi_{F,M})_n$ nth harmonic phase angles of F,M based on a cosine series, $(\bar{F},\bar{M}) = (\bar{F},\bar{M}) + \sum_{n=1}^{N} (F,M)_n \cos(n\theta - (\phi_{F,M})_n)$

ψ Pitch of hull, positive stern up

ψ_A Amplitude of hull pitch angle

Subscripts:

CW Value in calm water

Exp Experimental value

H Arising from hydrodynamic loading

h Value at hub radius

M Model value

MAX Maximum value

MIN Minimum value

p Port propeller

PEAK Peak value including variation of both time-average value per revolution and variation with blade angular position

s Starboard propeller

x,y,z Component in x,y,z direction

0.7 Value at r = 0.7R

ζ Value for operation in waves

ψ Value for operation with hull pitching motion

Superscripts:

$\bar{}$ Time-average value per revolution

$\tilde{}$ Unsteady value, peak value per revolution minus time-average value per revolution

$\dot{}$ Rate of change with time

Figure 1 - Hull and Propeller Geometry

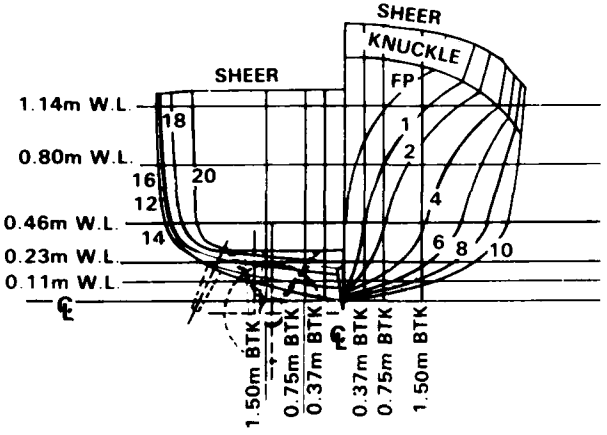

	MODEL	
LENGTH	6.10m	(20.0 ft)
LENGTH ON WATERLINE	5.70m	(18.7 ft)
LENGTH BETWEEN PERPENDICULARS	5.70m	(18.7 ft)
BEAM (MAXIMUM)	0.81m	(2.66 ft)
DRAFT (MEAN)	0.21m	(0.68 ft)
DISPLACEMENT	0.46 TONNES	(0.46 TONS)
WETTED SURFACE	3.17m^2	(50.2 ft^2)

APPENDAGES: SHAFTS, V-STRUTS, CENTERLINE SKEG, STABILIZER

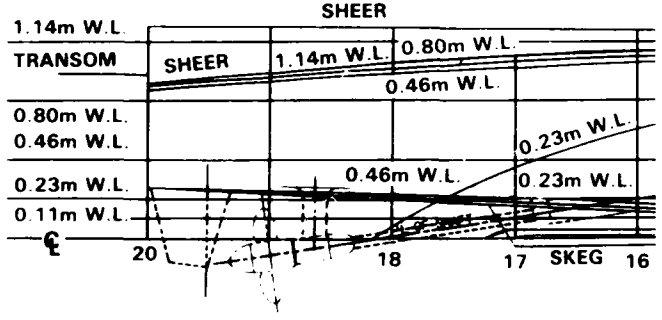

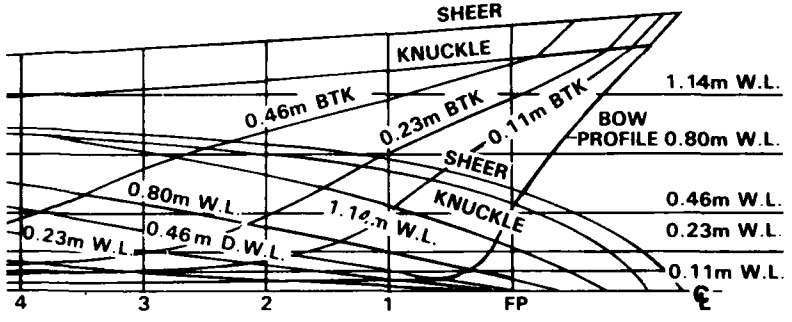

Figure 1a - Profile Lines and Body Plan

Figure 1 (Continued)

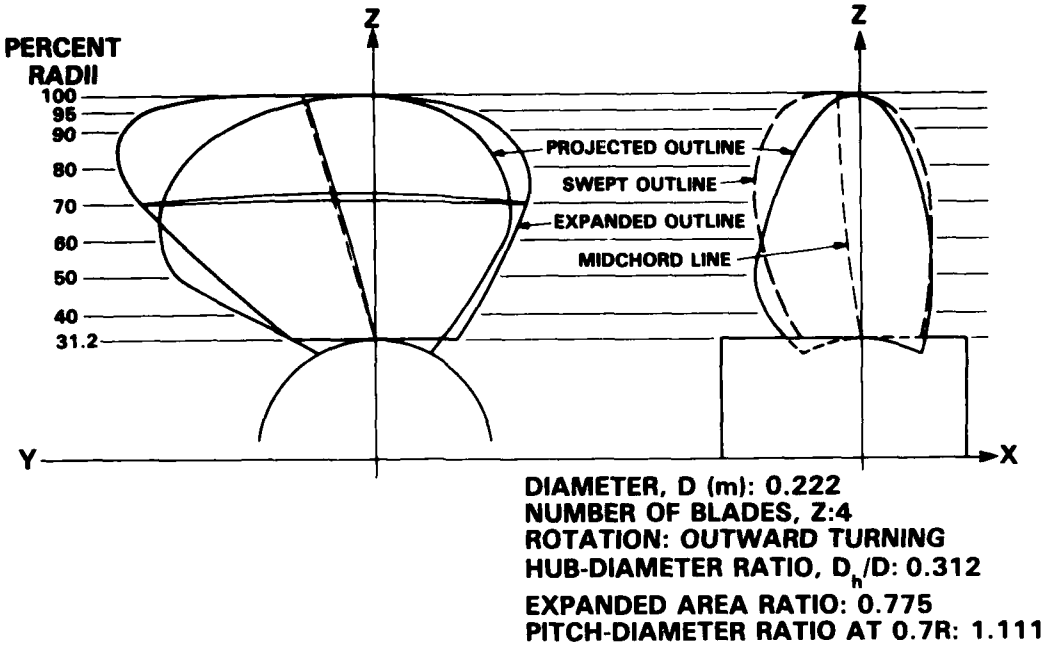

Figure 1b - Schematic Drawing of Propellers

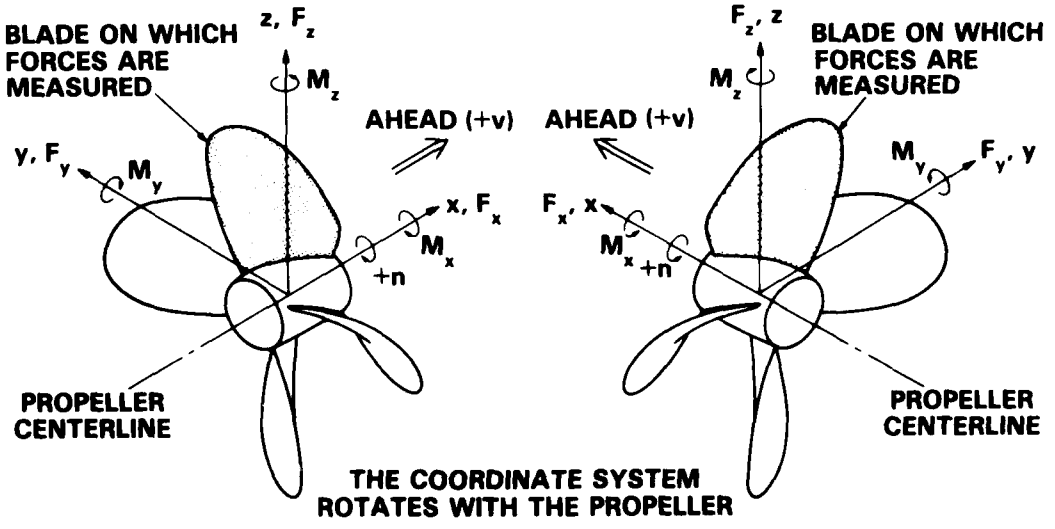

Figure 2 - Components of Blade Loading

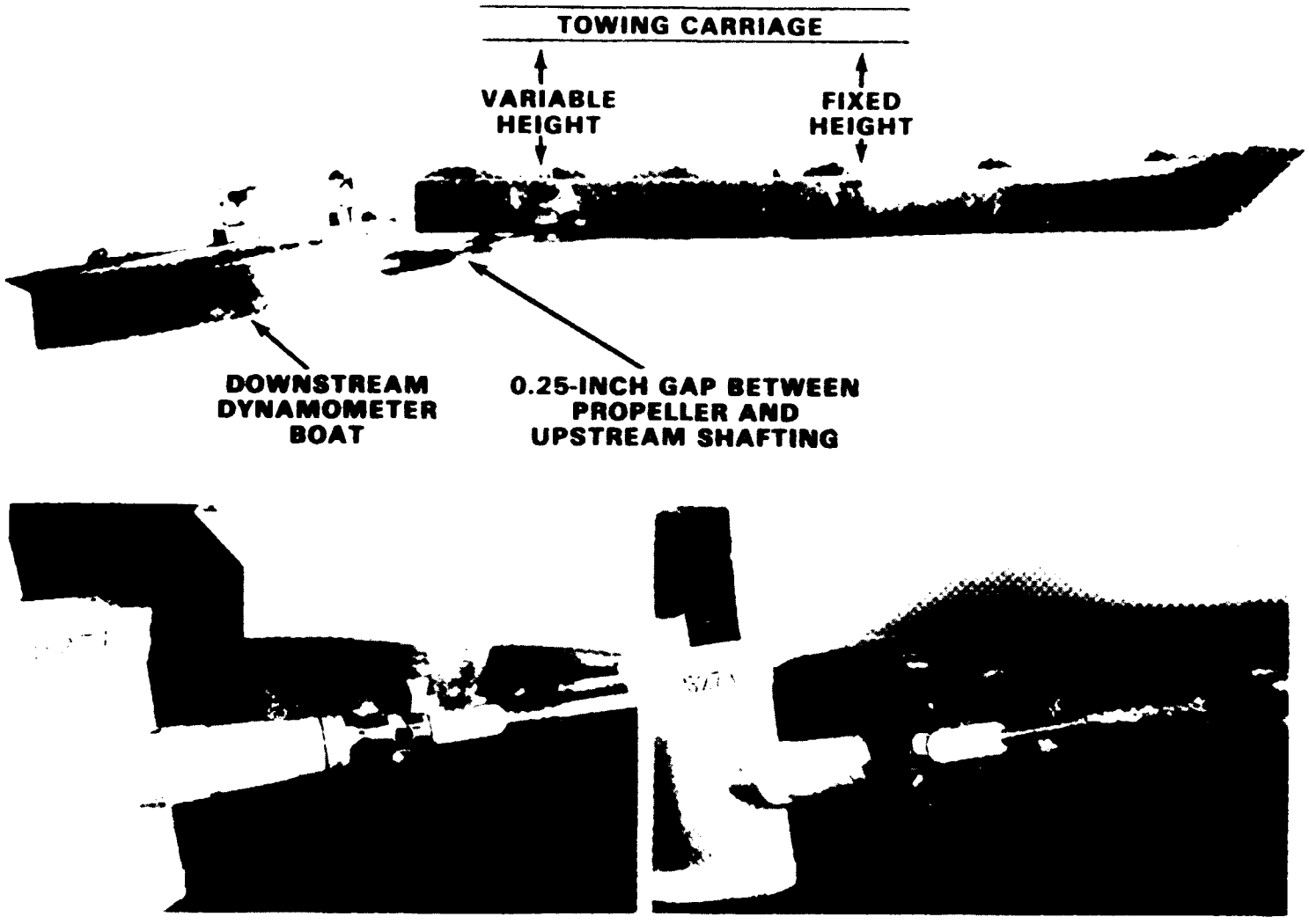

Figure 3 - Hull and Dynamometer Boat

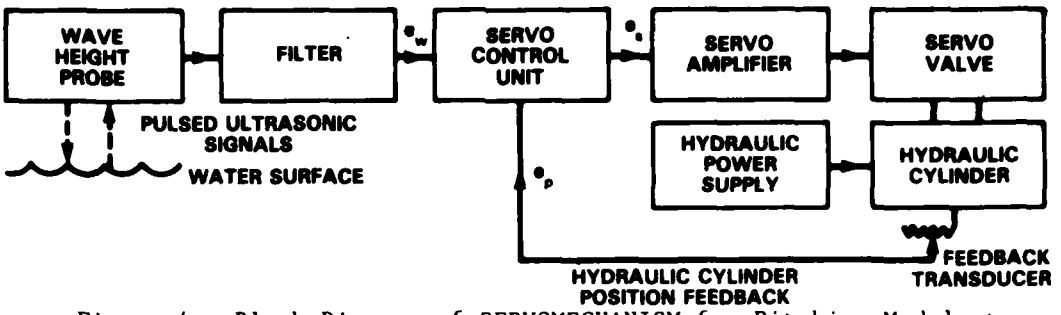

Figure 4 - Block Diagram of SERVOMECHANISM for Pitching Model at Specified Phase Relative to Waves

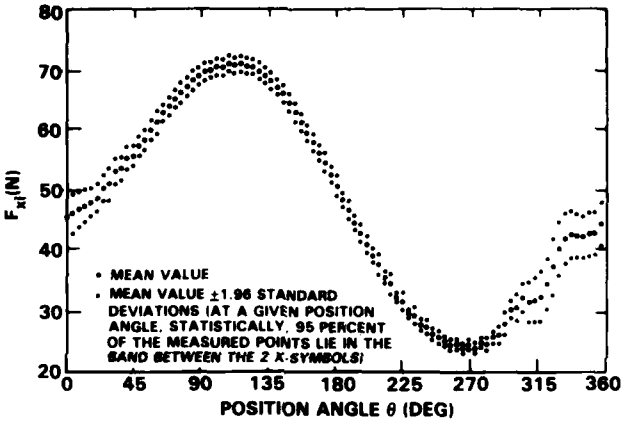

Figure 5 - Experimental Data Showing Plus and Minus 1.96 Standard Deviations on Measured Values of F_x

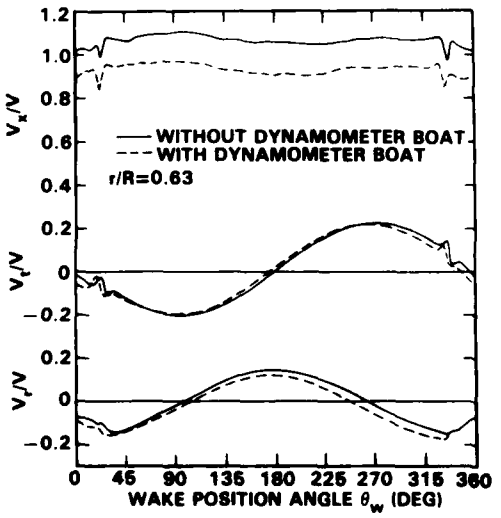

Figure 6a - r/R = 0.63

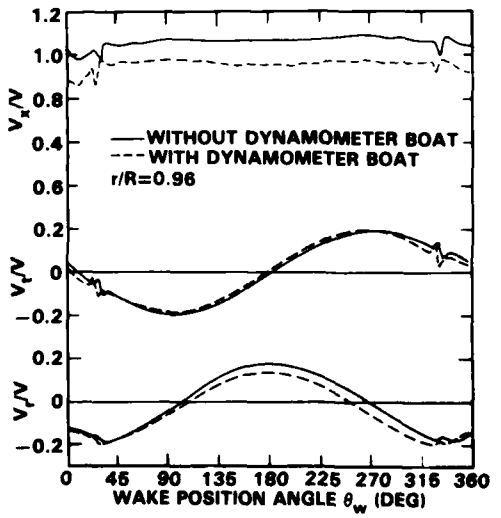

Figure 6b - r/R = 0.96

Figure 6 - Distribution of Wake in Propeller Plane

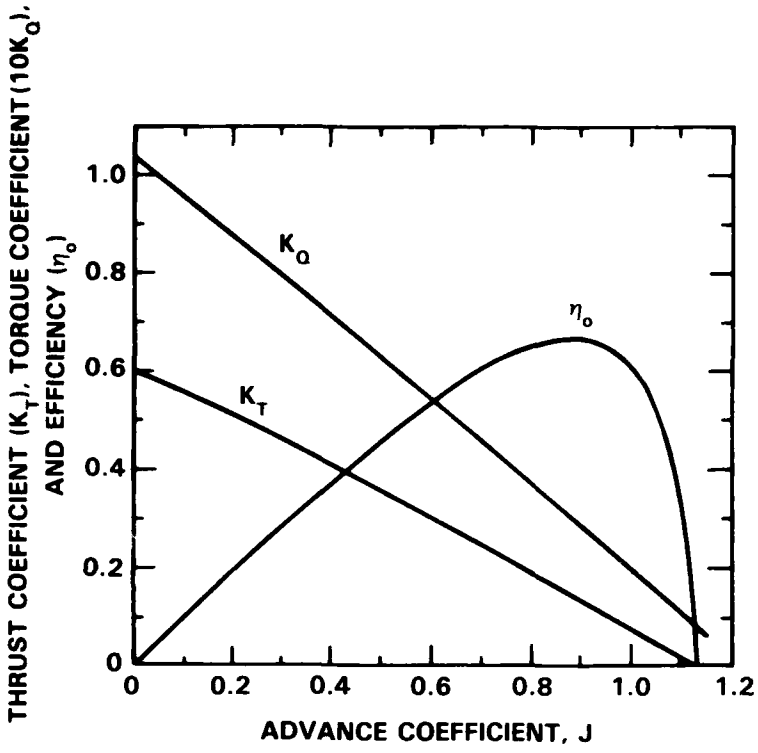

Figure 7 - Open-Water Characteristics of DTNSRDC Model Propellers 4710 and 4711

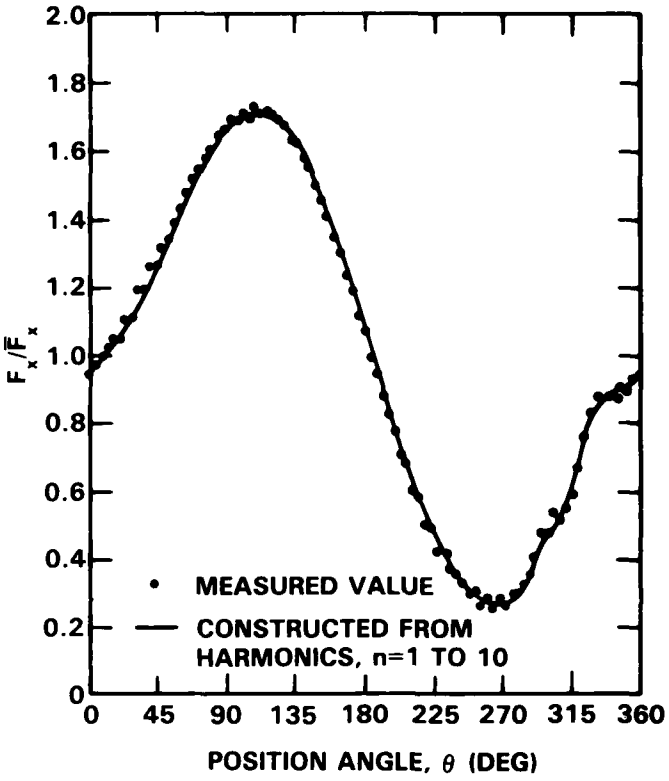

Figure 8 - Influence of Extraneous Signals on Measured Loads

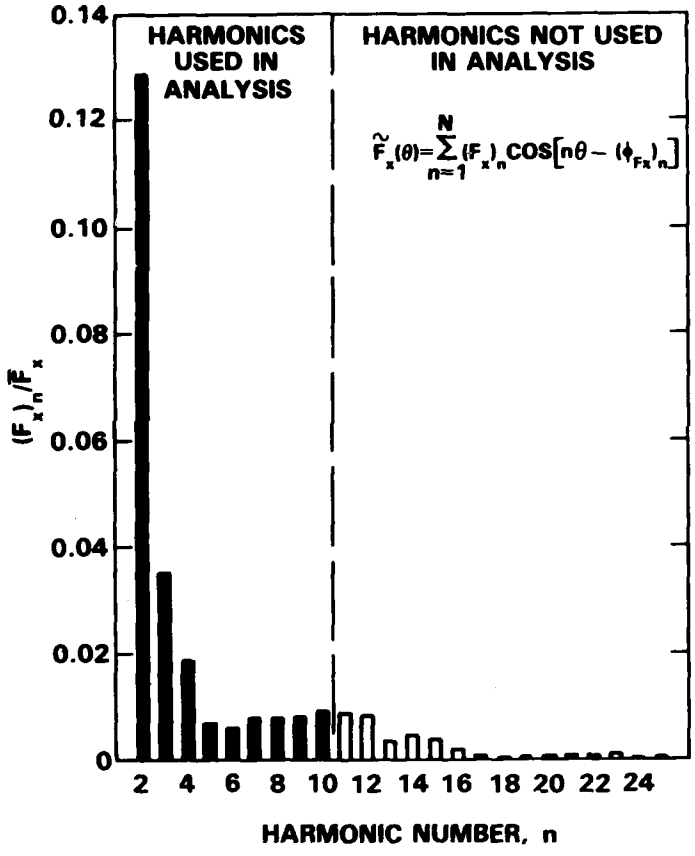

Figure 9 - Experimental Data Showing Extraneous Higher Harmonics

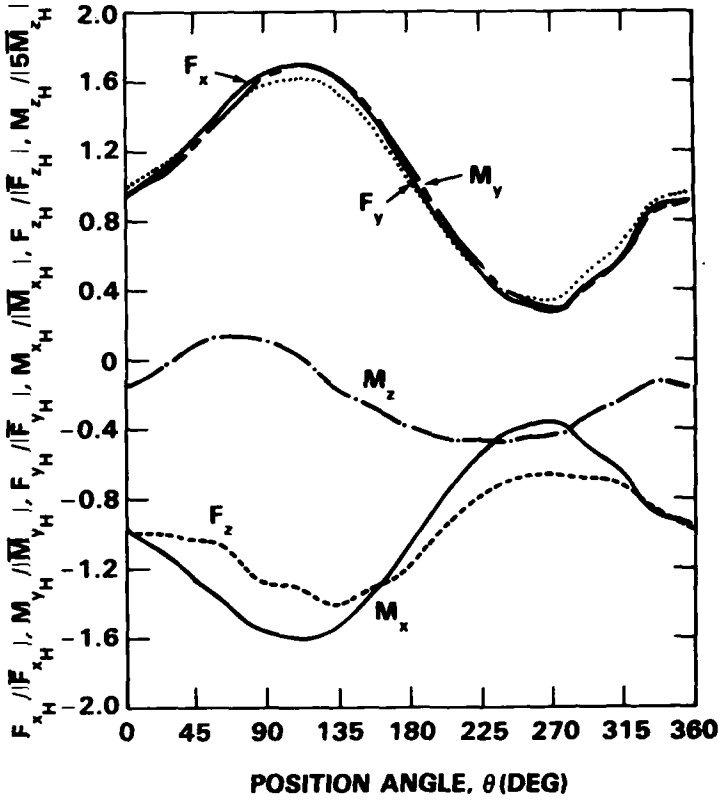

Figure 10 - Variation of Experimental Hydrodynamic Loads with Angular Position for Simulated Propulsion in Calm Water without Hull Pitching

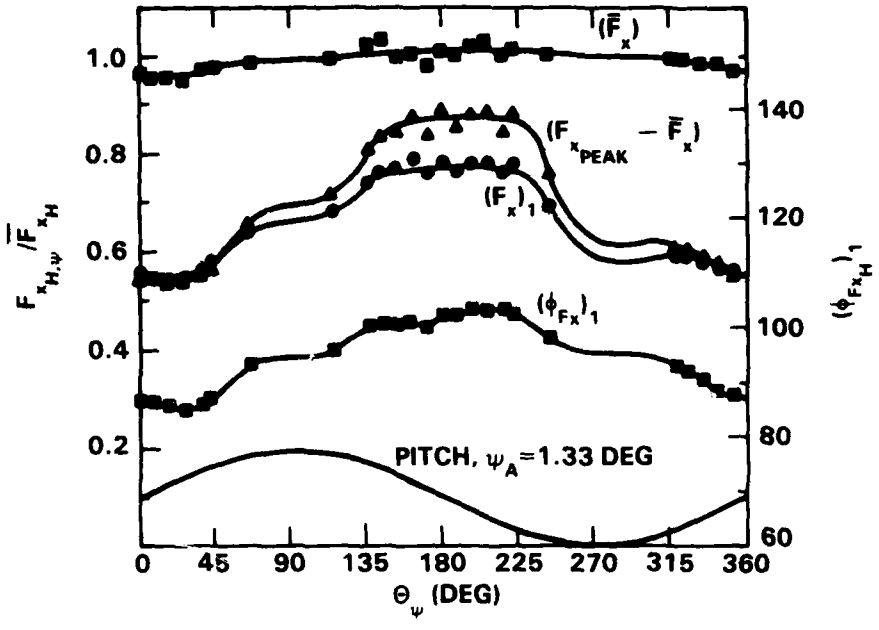

Figure 11a – F_x Component

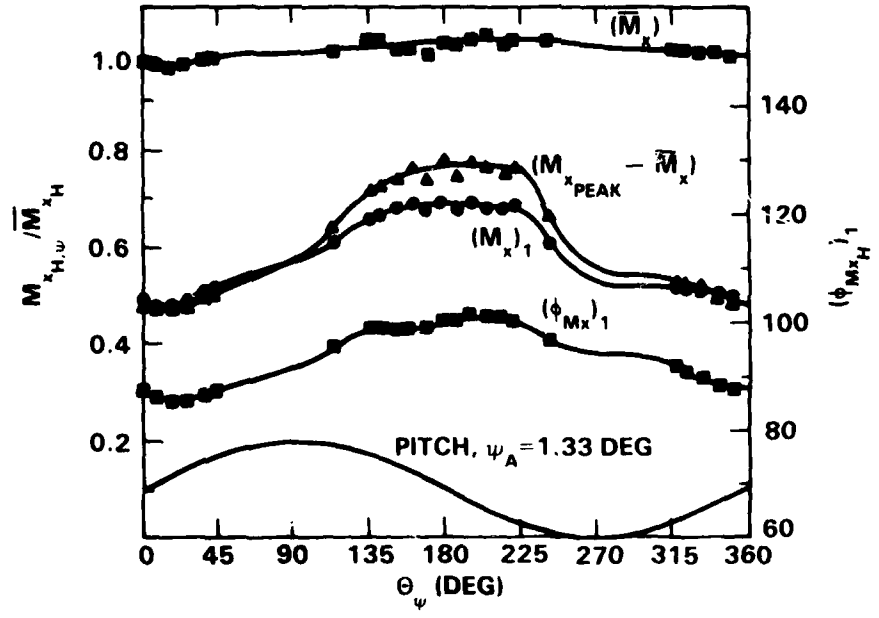

Figure 11b – M_x Component

Figure 11 - Variations of Hydrodynamic Loads with Hull Pitch Cycle for Operation in Calm Water

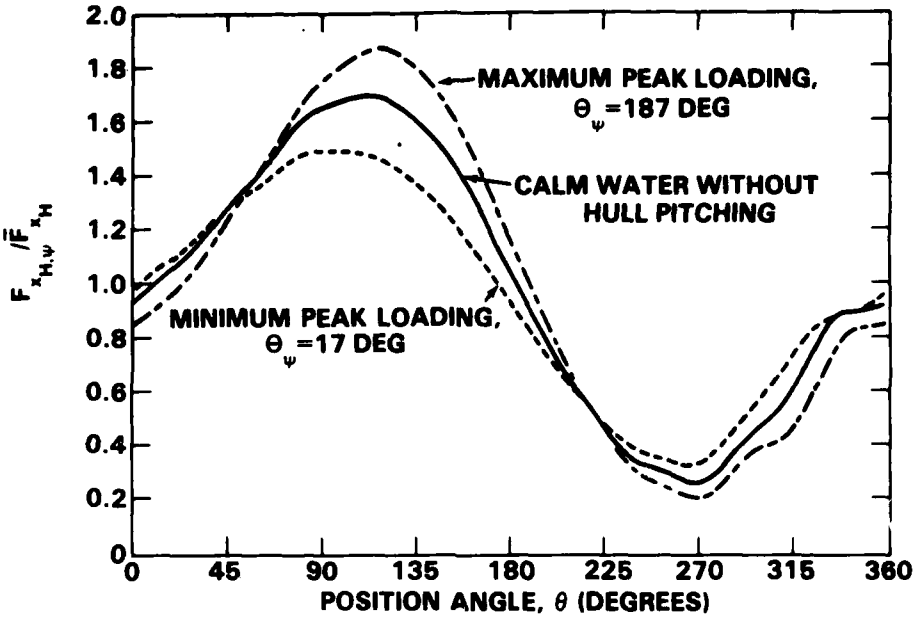

Figure 12 - Variation of F_x with Blade Angular Position for Hull Pitching in Calm Water Showing Portions of the Hull Pitch Cycle with Extremes of Peak Loading

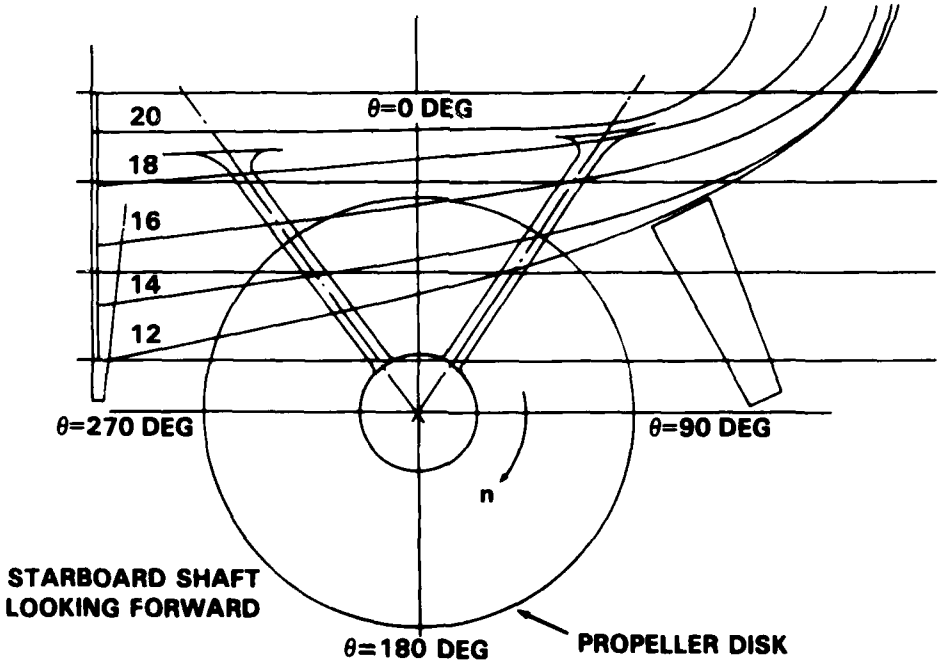

Figure 13 - Afterbody of Hull Showing Propeller Disk

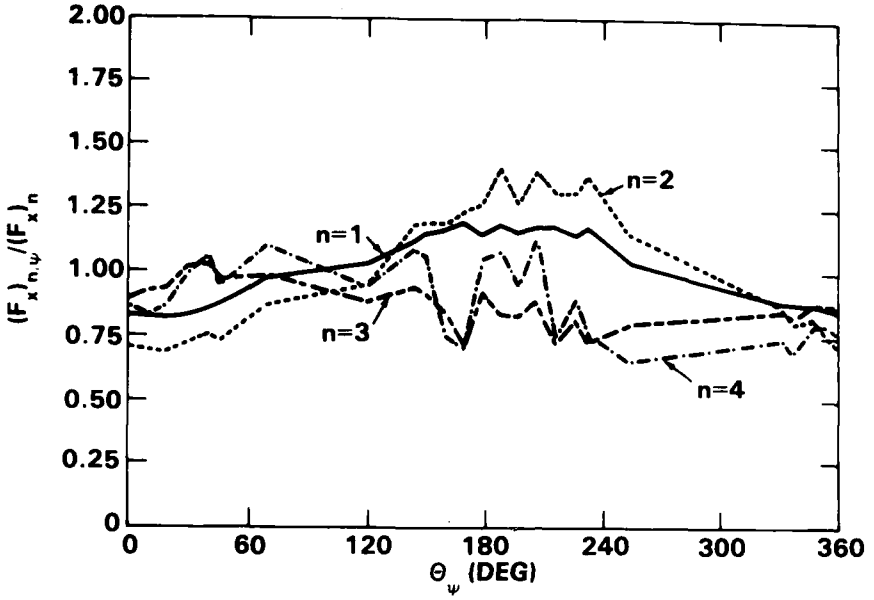

Figure 14a - Harmonics n - 1 to n 4

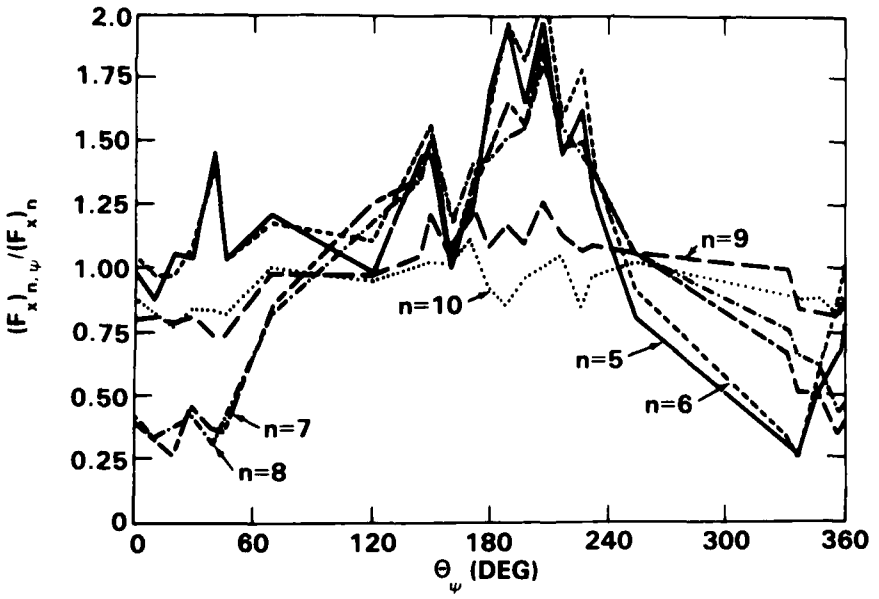

Figure 14b - Harmonics n 5 to n - 10

Figure 14 - Variations of the Harmonic Amplitudes of F_x During the Hull Pitch Cycle in Calm Water

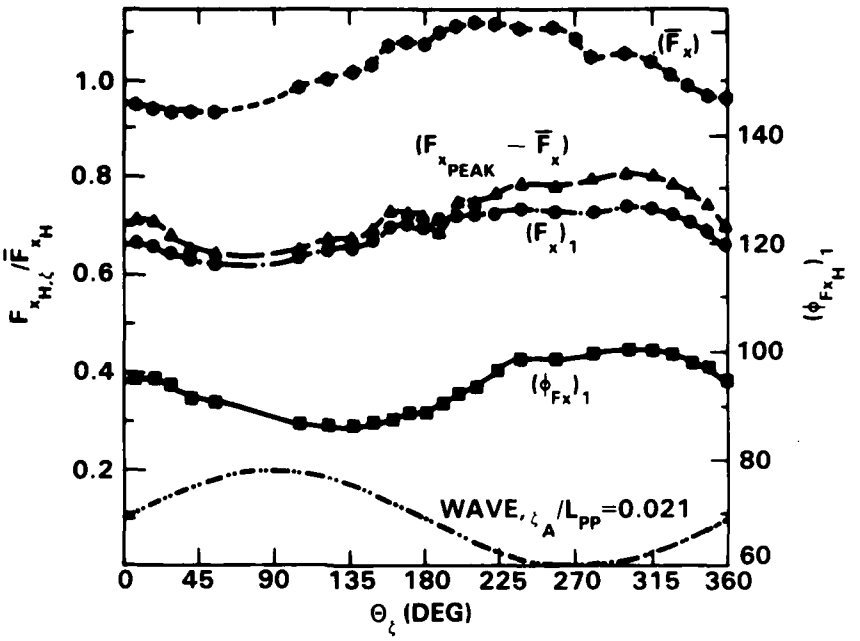

Figure 15a - F_X Component

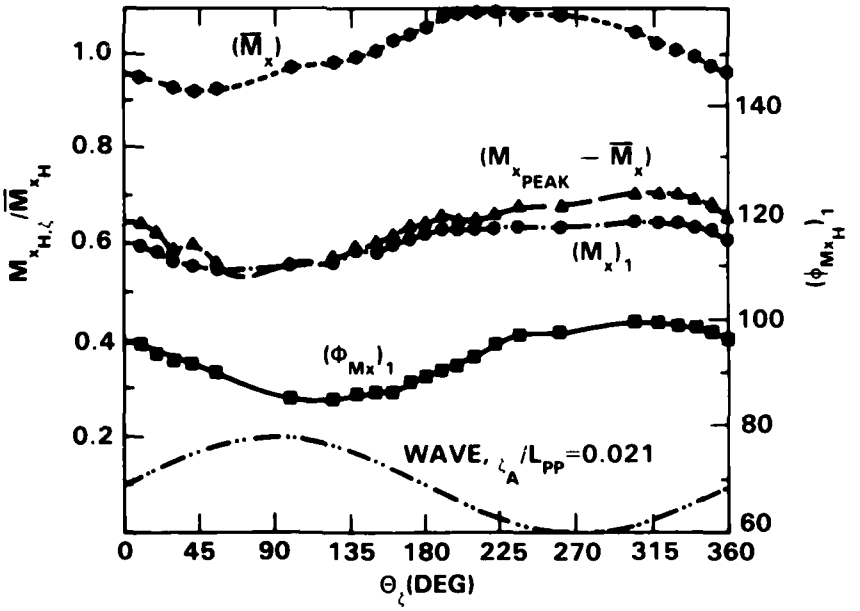

Figure 15b - M_X Component

Figure 15 - Variations of Hydrodynamic Loads with Location in Wave Cycle for Operation Without Hull Pitching

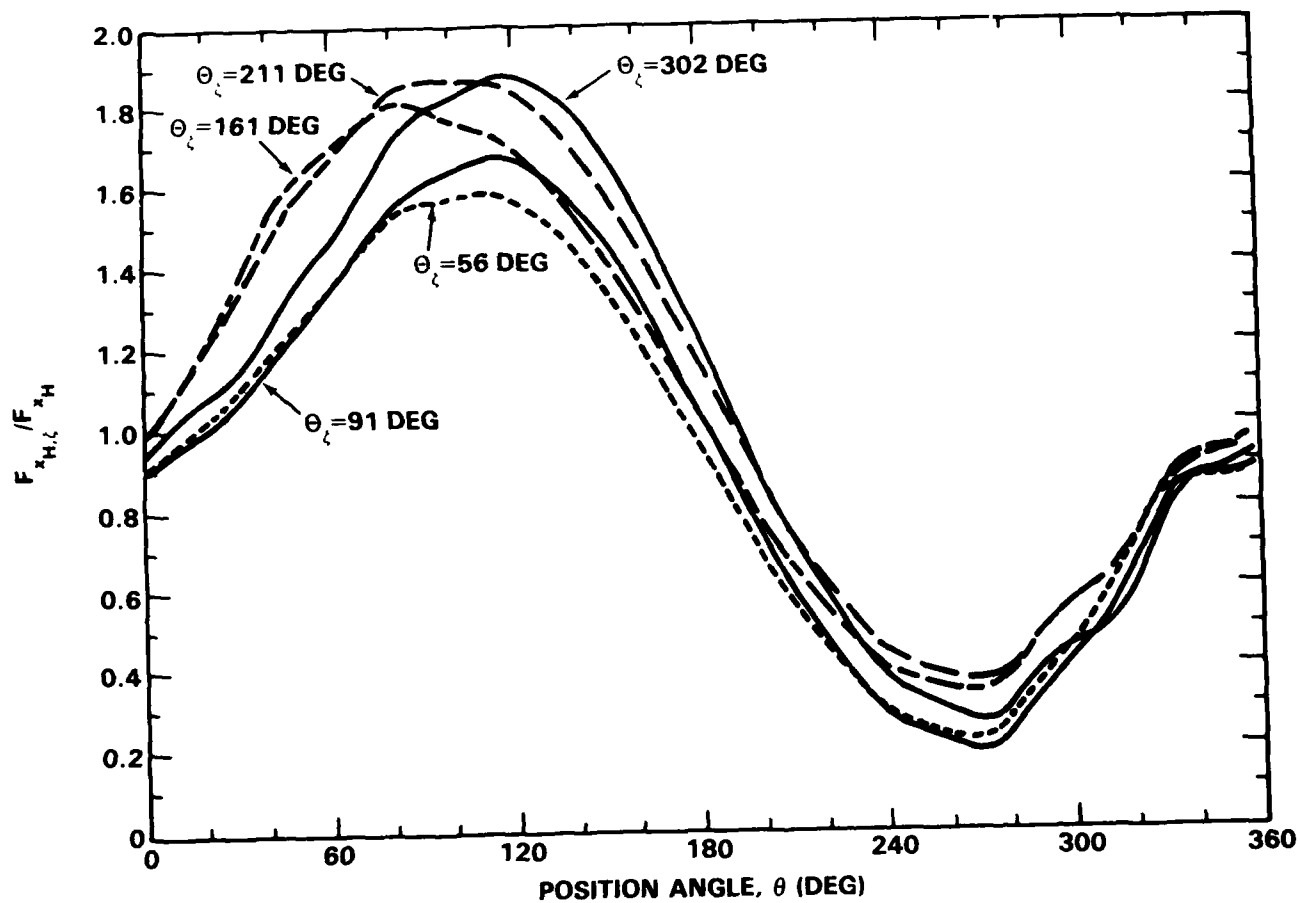

Figure 16 - Variation of F_x with Blade Angular Position for Operation in Waves Without Hull Pitching Showing Selected Locations in Wave Cycle Illustrating Extremes of Variation in Loading

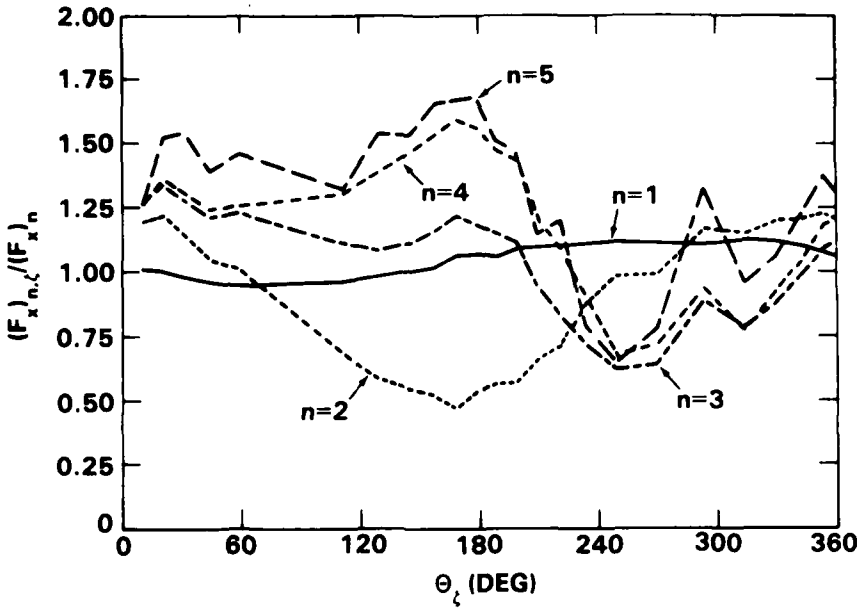

Figure 17a - Harmonics n = 1 to n = 5

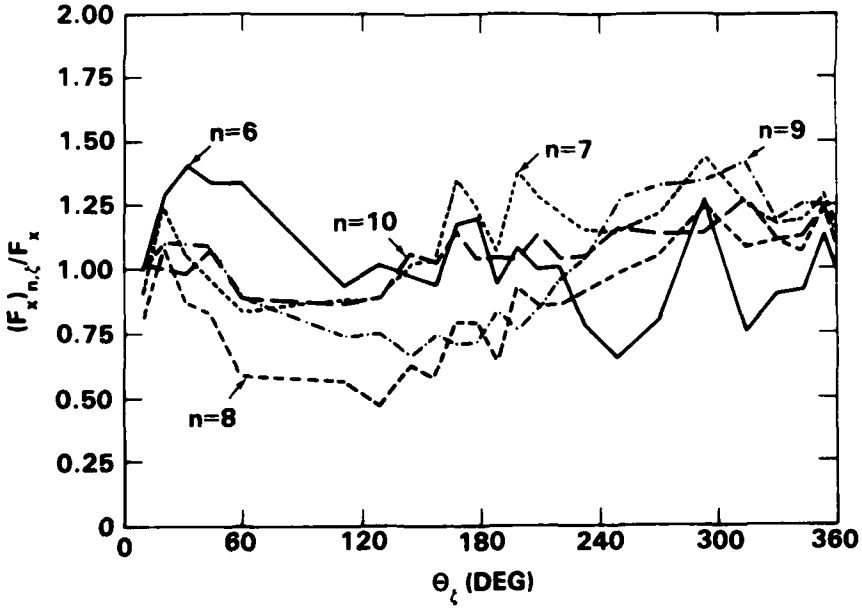

Figure 17b - Harmonics n = 6 to n = 10

Figure 17 - Variations of Harmonic Amplitudes of F_x During Wave Cycle Without Hull Pitching

Figure 18 - Comparison of Hydrodynamic Blade Loads for Operation in Waves with Hull Pitching with Values Obtained from Linear Superposition of Increases due to Pitching Only and Increases Due to Waves Only

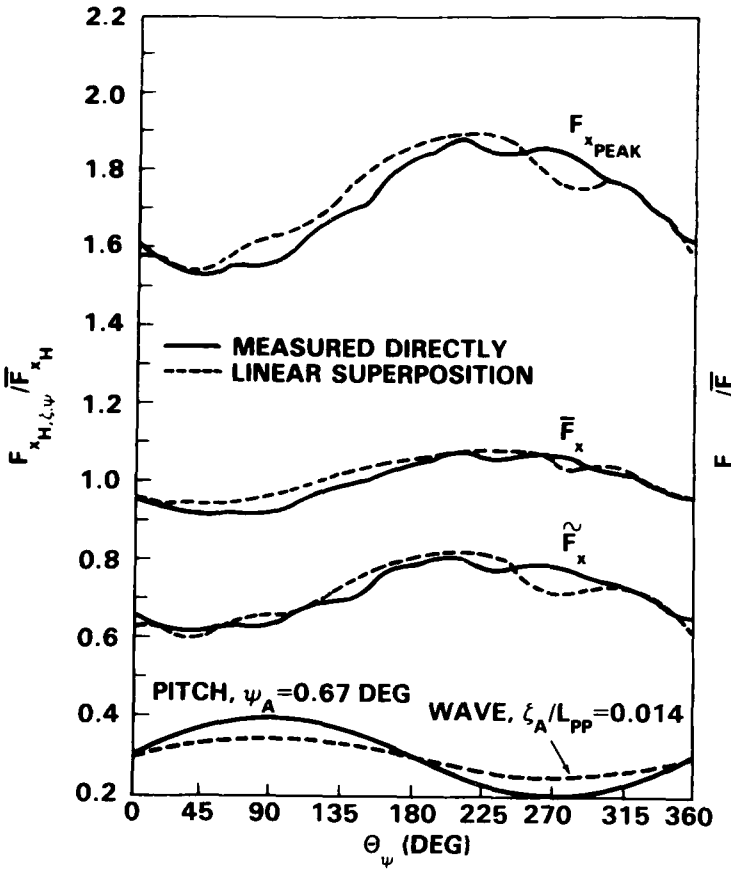

Figure 18a - $\Phi_\zeta - \Phi_\psi = 0$

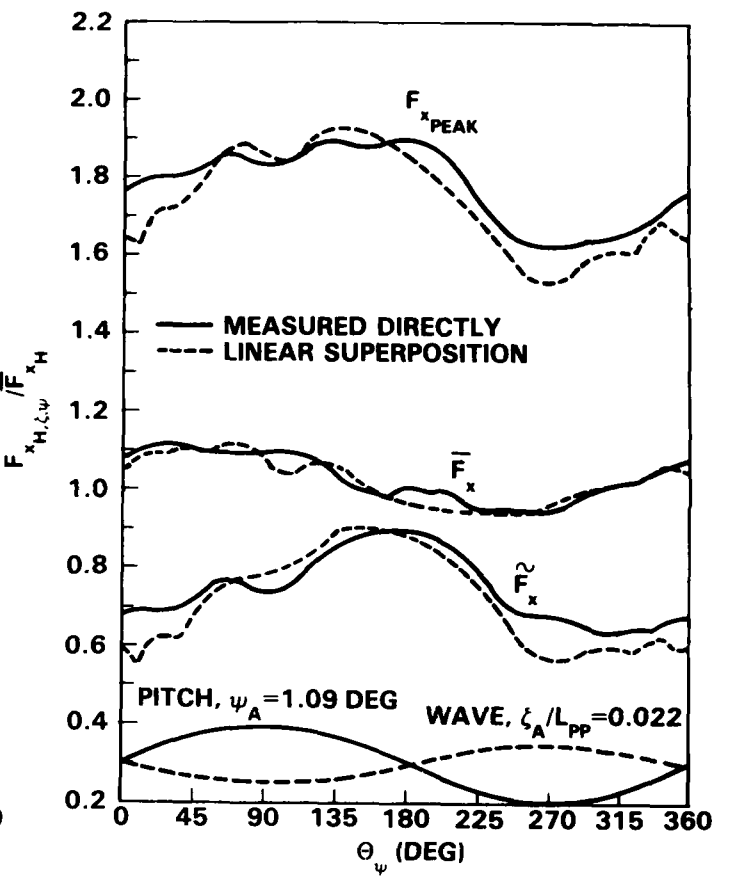

Figure 18b - $\Phi_\zeta - \Phi_\psi = 180$

Figure 18 (Continued)

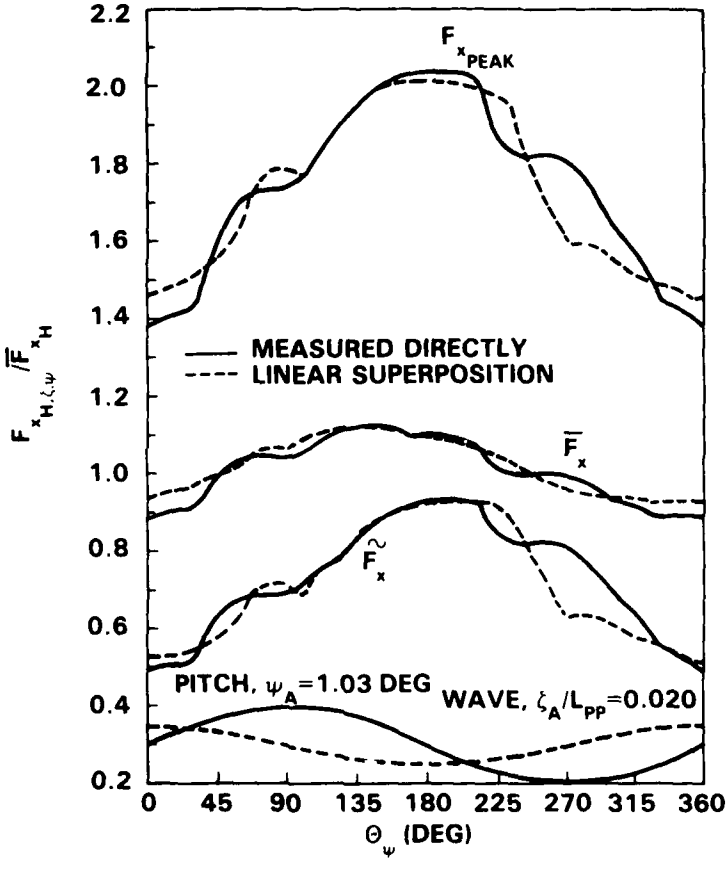

Figure 18c - $\Phi_\zeta - \Phi_\psi$ 90 degrees

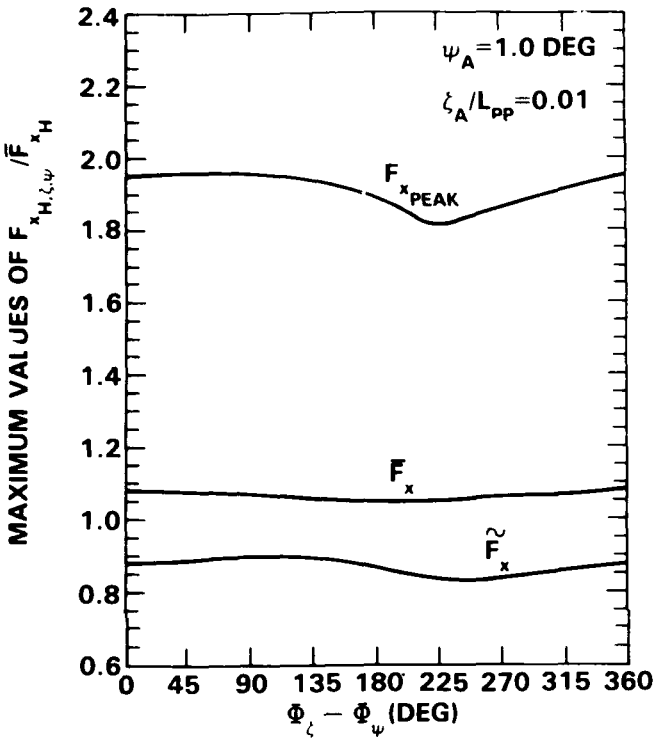

Figure 19a - ψ_A 1.0 deg, ζ_A/L_{PP} 0.01

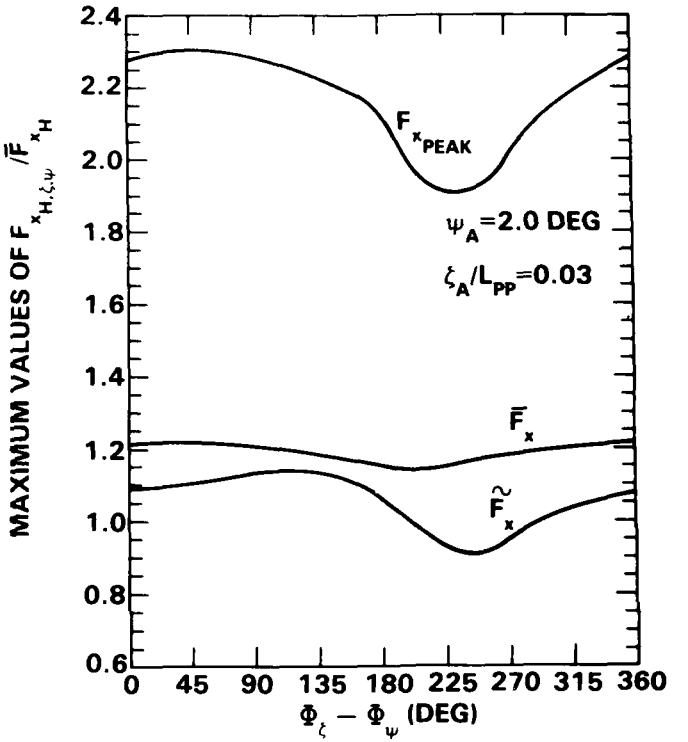

Figure 19b - ψ_A = 2.0 deg, ζ_A/L_{PP} = 0.03

Figure 19- Maximum Absolute Values of Blade Loads for Various Values of ψ_A, ζ_A/L_{PP} and $\Phi_\zeta - \Phi_\psi$ Derived from Linear Superposition of Increases due to Pitching Only and Increases due to Waves Only

Table 1 - Experimental Conditions

FOR ALL EXPERIMENTS: $V_M = 3.58$ m/s (6.96 knots)

$n_M = 18.80$ rps

$J_V = 0.86$

$(1 - w_T) = 1.00^*$

$J_T = 0.86^*$

+		ψ_A (DEG)	f_ψ (H_z)	$f_\psi\sqrt{L_{PP}/g}$	ζ_A/L_{PP}	f_ζ (H_z)	L_W/L_{PP}	$\Phi_\zeta - \Phi_\psi$
1	Calm Water without Hull Pitching	0	NA	NA	0	NA	NA	NA
2	Hull Pitching in Calm Water	1.33	0.80	2.63	0	NA	NA	NA
3	Waves without Hull Pitching	0	NA	NA	0.021	0.80	1.62	NA
4	Hull Pitching in Waves	0.67	0.80	2.63	0.014	0.80	1.62	0
5	Hull Pitching in Waves	1.09	0.80	2.63	0.022	0.80	1.62	180
6	Hull Pitching in Waves	1.03	0.80	2.63	0.020	0.80	1.62	90

* Effective value without dynamometer boat

\+ Number of Condition

Table 2 - Time-Average Hydrodynamic Loads for Operation in Calm Water without Hull Pitching*

$\bar{F}_x$	32.64 N +	7.338 LB ++	$\bar{K}_{Fx}$	0.0383 ++
$\bar{M}_y$	2.463 N-m +	21.801 IN-LB ++	$\bar{K}_{My}$	0.0130 ++
$\bar{F}_y$	19.92 N +	4.480 LB ++	$\bar{K}_{Fy}$	0.0234 ++
$\bar{M}_x$	− 1.549 N-m +	− 13.712 IN-LB ++	$\bar{K}_{Mx}$	−0.0082 ++
$\bar{F}_z$	− 25.47 N	− 5.725 LB	$\bar{K}_{Fz}$	− 0.0299
$\bar{M}_z$	− 0.194 N-m	− 1.719 IN-LB	$\bar{K}_{Mz}$	− 0.0010

* Condition 1 in Table 1

\+ Effective value without dynamometer boat

++ Corrected for influence of dynamometer boat

Table 3 - Comparison of Measured F_x with Other Transom-Stern Configurations for Operation in Calm Water with Hull Pitching

MODEL HULL	PRESENT MODEL TWIN-SCREW	SINGLE SCREW	TWIN-SCREW
Reference	–	Boswell et al (1976a, 1976b)	Jessup et al (1977) Boswell et al (1978)
Amplitude of Pitching, ψ_A (deg)	1.33	2.00	1.85
Period of Pitching T_ψ (sec)	1.25	1.25	1.25
Model speed, V_M (m/sec)	3.58	3.33	3.25
Maximum pitching velocity of propeller, V_ψ/V_M	0.082	0.145*	0.133
$(V_{t0.7})_1/V$	0.199	0.156	0.123
$[(V_{t0.7})_1+V_\psi]/(V_{t0.7})_1$	1.41	1.93*	2.08
$\tilde{F}_{x_{MAX,\psi}}/\bar{F}_x$	0.89	0.59	0.60
$(F_{x_{MAX}} - \bar{F}_x)/\bar{F}_x$	0.72	0.38	0.42
$\tilde{F}_{x_{MAX,\psi}}/(F_{x_{MAX}} - \bar{F}_x$	1.24	1.55	1.43
$[\tilde{F}_{x_{MAX,\psi}} - (\bar{F}_{x_{MAX}} - \bar{F}_x)]/\bar{F}_x$	0.17	0.21	0.18
$\bar{F}_{x_{MAX,\psi}}/\bar{F}_x$	1.03	1.03	1.10
$F_{x_{MAX}}/F_{x\psi}$	1.03	1.02	1.05
$\dfrac{\tilde{F}_{x_{MAX,\psi}}/(F_{x_{MAX}} - \bar{F}_x) - 1}{[(V_{t0.7})_1+V_\psi]/(V_{t0.7})_1 - 1}$	0.59	0.59	0.40

The subscript ψ refers to operation in calm water with hull pitching, whereas absence of the subscript ψ refers to operation in calm water without hull pitching.

The subscript MAX with superscript – indicates the maximum absolute value of the time-average load per revolution.

The subscript MAX with no superscript indicates the maximum absolute value of the peak load per revolution.

The subscript MAX with superscript ~ indicates the maximum absolute value of the peak minus time – average load per revolution.

* A numerical error was found in the values presented by Boswell et al (1976a, 1976b). This error has been corrected in the values presented in this Table.

Table 4 - Summary of Maximum Values of Hydrodynamic Loads for Operation in Calm Water with Hull Pitching

LOADING COMPONENT	F_{x_H}	M_{y_H}	F_{y_H}	M_{x_H}
$\bar{L}_{MAX,\psi}/\bar{L}$	1.03	1.04	1.04	1.05
$L_{MAX,\psi}/\bar{L}$	1.91	1.92	1.84	1.82
$L_{MAX}/\bar{L}$	1.71	1.70	1.62	1.61
$(L_{MAX,\psi} - \bar{L})/(L_{MAX} - \bar{L})$	1.28	1.31	1.35	1.34
$(L_{MAX,\psi} - L_{MAX})/\bar{L}$	0.20	0.22	0.22	0.21
$L_{MAX,\psi}/L_{MAX}$	1.12	1.13	1.14	1.13
$L_{MAX,\psi}/\bar{L}$	0.89	0.88	0.80	0.78
$\tilde{L}_{MAX,\psi}/(L_{MAX} - \bar{L})$	1.25	1.26	1.29	1.28
$(\tilde{L}_{MAX,\psi} - (L_{MAX} - \bar{L}))/\bar{L}$	0.18	0.18	0.18	0.17
$(L)_{1\ MAX,\psi}/\bar{L}$	0.79	0.77	0.73	0.69
$(L)_1/\bar{L}$	0.66	0.64	0.59	0.59
$(L)_{1MAX,\psi}/(L)_1$	1.20	1.20	1.24	1.17
$((L)_{1MAX,\psi} - (L)_1)/\bar{L}$	0.12	0.12	0.13	0.10
$\bar{L}$ (N OR N-m)	32.65	2.46	19.93	1.55

L refers to any one of the indicated loading components; i.e., F_x, M_y, F_y, M_x.

The subscript ψ refers to operation in calm water with hull pitching (Condition 2 in Table 1), whereas the absence of the subscript ψ refers to operation in calm water without hull pitching (Condition 1 in Table 1).

The subscript MAX with superscript — indicates the maximum absolute value of the time-average load per revolution.

The subscript MAX with no superscript indicates the maximum absolute value of the peak load per revolution.

The subscript MAX with superscript ~ indicates the maximum absolute value of the peak minus time-average load per revolution.

The subscript 1MAX indicates the maximum value of the first harmonic load per revolution.

Table 5 - Summary of Maximum Values of Hydrodynamic Loads for Operation in Waves without the Hull Pitching

LOADING COMPONENT	F_{x_H}	M_{y_H}	F_{y_H}	M_{x_H}
$\bar{L}_{MAX,\zeta}/\bar{L}$	1.12	1.14	1.08	1.09
$L_{MAX,\zeta}/\bar{L}$	1.90	1.92	1.77	1.77
$L_{MAX}/\bar{L}$	1.71	1.70	1.62	1.61
$(L_{MAX,\zeta} - \bar{L})/(L_{MAX} - \bar{L})$	1.27	1.31	1.24	1.26
$(L_{MAX,\zeta} - L_{MAX})/\bar{L}$	0.19	0.22	0.15	0.16
$L_{MAX,\zeta}/L_{MAX}$	1.11	1.13	1.09	1.10
$\bar{L}_{MAX,\zeta}/\bar{L}$	0.81	0.82	0.72	0.70
$\tilde{L}_{MAX,\zeta}/(L_{MAX} - \bar{L})$	1.14	1.17	1.16	1.15
$(\tilde{L}_{MAX,\zeta} - (L_{MAX} - \bar{L}))/\bar{L}$	0.10	0.12	0.10	0.09
$(L)_{1MAX,\zeta}/L$	0.74	0.73	0.67	0.65
$(L)_1/L$	0.66	0.64	0.59	0.59
$(L)_{1MAX,\zeta}/(L)_1$	1.12	1.14	1.14	1.10
$((L)_{1MAX,\zeta} - (L)_1)/\bar{L}$	0.08	0.09	0.08	0.06
$\bar{L}$ (N OR N-m)	32.65	2.46	19.93	1.55

L refers to any one of the indicated loading components; i.e., F_x, M_y, F_y, M_x.

The subscript ζ refers to operation in waves without hull pitching (Condition 3 in Table 1), whereas the absence of the subscript refers to operation in calm water without hull pitching (Condition 1 in Table 1).

The subscript MAX with superscript – indicates the maximum absolute value of the time-average load per revolution.

The subscript MAX with no superscript indicates the maximum absolute value of the peak load per revolution.

The subscript MAX with superscript $\sim$ indicates the maximum absolute value of the peak minus time-average load per revolution.

The subscript 1MAX indicates the maximum value of the first harmonic load per revolution.

INITIAL DISTRIBUTION

Copies	
1	ARMY CHIEF OF RES & DIV
1	ARMY ENGR R&D LAB
2	CHONR
	1 Code 438
	1 Lib
1	NRL
4	ONR BOSTON
4	ONR CHICAGO
4	ONR LONDON, ENGLAND
2	USNA
	1 Lib
	1 Johnson
1	NAVPGSCOL Lib
1	NROTC & NAVADMINU, MIT
1	NADC
5	NOSC
	1 1311 Lib
	1 6005
	1 13111 Lib
	1 2501/Hoyt
	1 Nelson
1	NWC
39	NAVSEA
	3 SEA 05H
	5 SEA 05R
	1 SEA 55
	3 SEA 55D
	1 SEA 55W
	3 SEA 56D
	1 SEA 56X
	3 SEA 56X1
	1 SEA 56X2
	3 SEA 56X4
	1 SEA 56X5

Copies	
39	NAVSEA (Continued)
	1 PMS-378
	1 PMS-380
	1 PMS-381
	1 PMS-383
	1 PMS-389
	1 PMS-391
	1 PMS-392
	1 PMS-393
	1 PMS-397
	1 PMS-399
	1 PMS-400
	1 SEA Tech Rep Bath, England
	2 DET NORFOLK (Sec 6660)
1	FAC 032C
1	MILITARY SEALIFT COMMAND (M-4EX)
1	NAVSHIPYD/PTSMH
1	NAVSHIPYD/PHILA
1	NAVSHIPYD/NORVA
1	NAVSHIPYD/CHASN
1	NAVSHIPYD/LBEACH
1	NAVSHIPYD/MARE
1	NAVSHIPYD/PUGET
1	NAVSHIPYD/PEARL
12	DTIC
2	HQS COGARD
1	US COAST GUARD (G-ENE-4A)
1	LC/SCI & TECH DIV
8	MARAD
	1 DIV SHIP DES
	1 COORD RES
	1 Schubert

Copies	
8	MARAD (Continued) 1 Falls 1 Dashnaw 1 Hammer 1 Lasky 1 Siebold
2	MMA 1 Lib 1 MARITIME RES CEN
2	NASA STIF 1 DIR RES
1	NSF ENGR DIV Lib
1	DOT Lib
1	U BRIDGEPORT/URAM
2	U CAL BERKELEY/DEPT NAME 1 NAME Lib 1 Webster
1	U CAL SAN DIEGO/ELLIS
2	UC SCRIPPS 1 Pollack 1 Silverman
1	U MARYLAND/GLEN MARTIN INST
1	U MISSISSIPPI/DEPT OF M.E.
4	CIT 1 AERO Lib 1 Acosta 1 Plesset 1 Wu
1	CATHOLIC U
1	COLORADO STATE U/Albertson
1	U CONNECTICUT/Scottron
1	CORNELL U/Sears
1	FLORIDA ATLANTIC U OE Lib

Copies	
3	HARVARD U 1 McKay Lib 1 Birkoff 1 Carrier
2	U HAWAII/Bretschneider
1	U ILLINOIS/Robertson
2	U IOWA 1 IHR/Kennedy 1 IHR/Landweber
2	Johns Hopkins U 1 Phillips 1 Inst Coop Res
1	U KANSAS CIV ENGR Lib
1	KANSAS ST U ENGR EXP/Lib
1	LEHIGH U FRITZ ENGR LAB Lib
1	LONG ISLAND U
3	U MICHIGAN/DEPT NAME 1 NAME Lib 1 Parsons 1 Vorus
6	MIT 1 BARKER ENGR Lib 2 OCEAN ENGR/Kerwin 1 OCEAN ENGR/Leehey 1 OCEAN ENGR/Newman 1 OCEAN ENGR/Burke
3	U MINNESOTA SAFHL 1 Killen 1 Song 1 Wetzel
2	STATE U MARITIME COLL S U ARL Lib 1 ENGR DEPT 1 INST MATH SCI
1	NOTRE DAME ENGR Lib

Copies	
5	PENN STATE U ARL 1 Lib 1 Henderson 1 Gearhart 1 Parkin 1 Thompson
1	PRINCETON U/Mellor
1	RENSSELAER/DEPT MATH
1	ST JOHNS U
1	VIRGINIA TECH
3	SWRI 1 APPLIED MECH REVIEW 1 Abramson 1 Burnside
1	BOEING ADV AMR SYS DIV
3	BOLT BERANEK AND NEWMAN 1 Brown 1 Jackson 1 Greeley
1	BREWER ENGR LAB
1	CAMBRIDGE ACOUS/Junger
1	CALSPAN, INC/Ritter
1	STANDFORD U/Ashley
1	STANDFORD RES INST Lib
3	SIT DAVIDSON LAB 1 Lib 1 Breslin 1 Tsakonas
1	TEXAS U ARL Lib
1	UTAH STATE U/Jeppson
2	WEBB INST 1 Ward 1 Hadler

Copies	
1	WHOI OCEAN ENGR DEPT
1	WPI ALDEN HYDR LAB Lib
1	ASME/RES COMM INFO
1	ASNE
1	SNAME
1	AERO JET-GENERAL/Beckwith
1	ALLIS CHALMERS, YORK, PA
1	AVCO LYCOMING
1	BAKER MANUFACTURING
2	BATH IRON WORKS CORP 1 Hansen 1 FFG7 PROJECT OFFICE
1	BETHLEHEM STEEL SPARROWS
3	BIRD-JOHNSON CO 1 Case 1 Ridley 1 Norton
2	DOUGLAS AIRCRAFT 1 TECHNICAL Lib 1 Smith
2	EXXON RES DIV 1 Lib 1 Fitzgerald
1	FRIEDE & GOLDMAN/Michel
1	GEN DYN CONVAIR ASW-MARINE SCIENCES
3	GIBBS & COX 1 TECH Lib 1 Olson 1 CAPT Nelson
1	GRUMMAN AEROSPACE/Carl

Copies	
3	HYDRONAUTICS 1 Etter 1 Scherer 1 Lib
1	INGALLS SHIPBUILDING
1	INST FOR DEFENSE ANAL
1	ITEK VIDYA
1	LITTLETON R & ENGR CORP/Reed
1	LITTON INDUSTRIES
1	LOCKHEED/Waid
1	MARITECH, INC/Vassilopoulis
2	HYDRODYNAMICS RESEARCH ASSOCIATES, INC 1 Cox 1 Valentine
1	NATIONAL STEEL & SHIPBLDG
1	NEWPORT NEWS SHIPBLDG Lib
1	NIELSEN ENGR/Spangler
1	HYDROMECHANICS, INC/Kaplin
1	NAR SPACE/Ujihara
3	ORI, INC 1 Bullock 1 Schneider 1 Kobayashi
1	PROPULSION DYNAMICS, INC
1	PROPULSION SYSTEMS, INC
1	SCIENCE APPLICATIONS, INC/Stern
1	GEORGE G. SHARP
1	SPERRY SYS MGMT Lib/Shapiro

Copies	
1	SUN SHIPBLDG 1 Lib
1	ROBERT TAGGART
2	TETRA TECH PASADENA 1 Chapkis 1 Furuya
1	TRACOR
1	UA HAMILTON STANDARD/Cornell

CENTER DISTRIBUTION

Copies	Code	Name
1	0120	Jewell
1	11	Ellsworth
1	1102.1	Nakonechny
1	15	Morgan
1	1506	Reed
1	1509	Powell
1	152	Lin
1	1521	Day
1	1521	Karafiath
1	1521	Hurwitz
1	1522	Dobay
1	1522	Remmers
1	1522	Wilson
1	154	McCarthy
1	1540.2	Cumming
1	1542	Huang
1	1542	Shen
1	1543	Jeffers
1	1543	Platzer
1	1543	Santore
1	1543	Wisler
1	1544	Brockett
30	1544	Boswell
1	1544	Caster

Copies	Code	Name
1	1544	Fuhs
20	1544	Jessup
1	1544	Kim
1	156	Cieslowski
1	1561	Feldman
1	1561	O'Dea
1	1562	Moran
1	1563	Smith
1	1564	Cox
1	172	Krenzke
1	1720.6	Rockwell
1	19	Sevik
1	19	Strasberg
1	1903	Chertock
1	1905	Blake
1	1942	Archibald
1	1962	Zaloumis
1	1962	Noonan
1	2814	Czyryca
10	5211.1	Reports Distribution
1	522.1	Lib (C)
1	522.2	Lib (A)

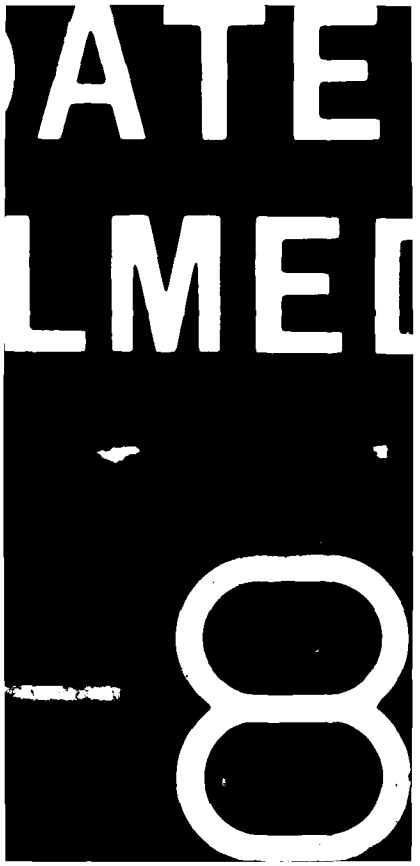
ATE
LME
8